Morphometry and pattern of a large sample (>20,000) of Canadian eskers and implications for subglacial drainage beneath ice sheets

CrossMark

Robert D. Storrar[*], Chris R. Stokes, David J.A. Evans

Department of Geography, Durham University, Durham, DH1 3LE, UK

ABSTRACT

Ice sheet flow is strongly influenced by the nature and quantity of meltwater entering the subglacial system. Accessing and monitoring contemporary drainage systems beneath ice sheets is notoriously difficult, but it is possible to utilise the exposed beds of palaeo-ice sheets. In particular, eskers record deposition in glacial drainage channels and are widespread on the exposed beds of former ice sheets. However, unlike some other common glacial landforms (e.g. drumlins) there have been relatively few attempts to investigate and quantify their characteristics at the ice sheet scale. This paper presents data on the distribution, pattern, and morphometry of a large (>20,000) sample of eskers in Canada, formed under the Laurentide Ice Sheet, including quantification of their length, fragmentation, sinuosity, lateral spacing, number of tributaries, and downstream elevation changes. Results indicate that eskers are typically very long (hundreds of km) and often very straight (mean sinuosity approximates 1). We interpret these long esker systems to reflect time-transgressive formation in long, stable conduits under hydrostatic pressure. The longest eskers (in the Keewatin sector) are also the least fragmented, which we interpret to reflect formation at an ice margin experiencing stable and gradual retreat. In many locations, the lateral distance between neighbouring eskers is remarkably consistent and results indicate a preferred spacing of around 12 km, consistent with numerical models which predict esker spacing of 8–25 km. In other locations, typically over soft sediments, eskers are rarer and their patterns are more chaotic, reflecting fewer large R-channels and rapidly changing ice sheet dynamics. Comparison of esker patterns with an existing ice margin chronology reveals that the meltwater drainage system evolved during deglaciation: eskers became more closely spaced with fewer tributaries as deglaciation progressed, which has been interpreted to reflect increased meltwater supply from surface melt. Eskers show no preference to trend up or down slopes, indicating that ice surface was an important control on their location and that the conduits were, in places, close to ice overburden pressure.

© 2014 The Authors. Published by Elsevier Ltd. This is an open access article under the CC BY license (http://creativecommons.org/licenses/by/3.0/).

1. Introduction

Eskers are elongate, straight-to-sinuous ridges of glaciofluvial sand and gravel, deposited predominantly in pressurised subglacial channels (Banerjee and McDonald, 1975; Brennand, 2000), but also connected to englacial and supraglacial tunnel systems (Price, 1969; Gustavson and Boothroyd, 1987). They are common in formerly warm-based glaciated terrains (e.g. Prest et al., 1968; Clark et al., 2004; Aylsworth et al., 2012; Storrar et al., 2013), making them a useful indicator of subglacial meltwater drainage pathways. Meltwater drainage beneath ice sheets is of fundamental importance to our understanding of ice dynamics. An increased supply of meltwater to the bed may help lubricate ice flow, resulting in an increase in ice velocity (e.g. Zwally et al., 2002; Joughin et al., 2008; Bartholomew et al., 2010; but see Schoof, 2010; Sundal et al., 2011). However, the nature of the drainage system is also important, with inefficient (distributed) systems of shallow water films and canals typically associated with higher ice velocities, and more organised and efficient systems with large channels typically associated with lower velocities (Nienow et al., 1996; Bartholomew et al., 2010). These drainage systems also have implications for sediment deformation and its impact on ice flow, because the mechanical properties of deformable till may be modified by water draining through it (Tulaczyk et al., 2000; Boulton et al., 2001). It is important, therefore, to understand how water is routed through subglacial drainage systems.

Unfortunately, direct observation of the subglacial drainage systems beneath modern ice sheets is extremely difficult. Thus,

* Corresponding author. Now at School of Geography, Queen Mary University of London, Mile End Road, London, E1 4NS, UK. Tel.: +44 (0) 20 7890 2751.
E-mail address: r.storrar@qmul.ac.uk (R.D. Storrar).

indirect methods such as dye tracing (e.g. Nienow et al., 1996), remote sensing (e.g. Fricker et al., 2010), numerical modelling (e.g. Lewis and Smith, 2009; Hewitt, 2013) and geophysical surveys (e.g. Carter et al., 2009) are employed to investigate how they operate beneath contemporary ice sheets. Whilst significant breakthroughs have been made with these techniques (e.g. Richards et al., 1996; Nienow et al., 1998; Wingham et al., 2006; Fricker et al., 2007), they are often limited by their spatial and temporal resolution. Indeed, numerical modelling of subglacial drainage systems is difficult because there are so few data with which to test model predictions, e.g. of channel spacing (Hewitt, 2011) and sinuosity (Schuler and Fischer, 2009). The abundance of eskers on palaeo-ice sheet beds provides huge potential to record aspects of subglacial meltwater drainage that are otherwise difficult or impossible to investigate using existing techniques.

To date, no large-scale, systematic quantification of the spatial patterns and morphometry of eskers has been undertaken. The aim of this paper is to address this shortfall by producing the first large-scale quantitative analysis of the patterns and spatial characteristics of eskers across an ice sheet bed, similar to those recently undertaken for ribbed moraine (Dunlop and Clark, 2006); drumlins (Clark et al., 2009) and mega-scale glacial lineations (Stokes et al., 2013; Spagnolo et al., 2014). This is achieved using a GIS dataset of eskers mapped from Landsat 7 ETM+ imagery of the whole of Canada, and covering almost 10,000,000 km^2 formerly occupied by the Laurentide Ice Sheet (LIS). These data are available as a map (Storrar et al., 2013), and were recently used to identify changes in esker density which may be associated with climatic changes (Storrar et al., 2014). Here, we build on this work and analyse esker patterns, distribution, length, fragmentation, sinuosity, spacing, tributaries, 'stream' ordering and slope, thereby providing an important dataset for testing both conceptual and numerical models of esker formation and providing new insights into channelised meltwater drainage at the ice sheet scale.

2. Definitions and previous work on esker morphometry and pattern

Aspects of esker pattern and morphometry have been reported previously, albeit for typically rather small sample sizes (e.g. $n < 100$). In this section, we provide a brief overview of previous work on esker morphometry and outline some important definitions of their morphometry and pattern that we report in this study. First and foremost, we use the term *esker ridge* to refer to individual ridges. Where several e*sker ridges* are aligned and clearly related to each other, but with intermittent gaps, we term them *eskers*. *Eskers*, in turn, form subsets of *esker systems*, which are comprised of *trunk eskers*, into which *tributary eskers* merge. *Esker systems* are analogous to a drainage basin.

2.1. Pattern and distribution

The heterogeneous distribution of eskers deposited beneath the LIS has been discussed by several authors, who have proposed genetic models to explain their variability (e.g. Shilts et al., 1987; Aylsworth and Shilts, 1989a; Clark and Walder, 1994). A seminal paper by Clark and Walder (1994), showed that eskers formed by the LIS and European Ice Sheets are prolific on the more resistant crystalline shield rocks and rare over less resistant sedimentary, and potentially deformable, substrates. They suggested that, over more resistant substrates, eskers are more likely to form in channels which are incised into the ice (R-channels) rather than into the substrate (N-channels). Others, however, have noted that eskers are present in areas of deformable substrates (e.g. Wright, 1973; Mooers, 1989), and that channelised systems may develop

over deformable materials (Shoemaker, 1986). Observations of eskers ending abruptly over relatively rigid Devonian carbonates in western Canada led Grasby and Chen (2005) to suggest that esker distribution in Canada is controlled by bedrock permeability, where preferential subglacial recharge through carbonate outcrop belts inhibits esker formation as water is readily drained through the subsurface. In contrast, the low-permeability rocks of the Canadian Shield enable high pressure water to exist at the base of the ice sheet, and thus form eskers. This is similar to a model put forward by Boulton and co-workers (Boulton et al., 2007a, b, 2009), who related esker spacing to the hydrogeological properties of the substrate. This is discussed further in Section 5.4.

Others have noted the similarity of esker patterns to fluvial systems: eskers in the Keewatin sector of the LIS, for example, are reminiscent of integrated Hortonian drainage networks and are seen to radiate outwards from the final location of the ice divide (Shilts et al., 1987; Aylsworth and Shilts, 1989a). More recently, Storrar et al. (2014) examined the pattern of eskers and found that esker density increases towards the locations of the final remnants of the ice sheet, which they related to increased meltwater supply from surface melting during deglaciation.

2.2. Length and fragmentation

Esker length (here given the notation l_e) is the distance covered by the crestline of an esker (Fig. 1A), and is related to the length of the conduit in which it is formed. Eskers are frequently described as forming fragmented systems (e.g. Fig. 2A) which can extend for several hundred km (e.g. Banerjee and McDonald, 1975; Aylsworth and Shilts, 1989a; Boulton et al., 2009). Our preliminary analysis of previously published maps of 846 esker ridges in the UK and 817 on the Kola Peninsula, Russia (Clark et al., 2004; Hättestrand and Clark, 2006) reveal that the length of esker ridges in these areas do not follow a normal distribution, but are strongly positively skewed (see Fig. 3A). Individual esker ridges average between 1 km and 3 km long, and extend up to a maximum of 18.2 km in the UK and 9.9 km in the Kola Peninsula.

2.3. Sinuosity

Esker ridge sinuosity (S; Fig. 1B) is expressed as the ratio between the length of the esker ridge (l_e) and the length of a straight line between the beginning and end points of the esker ridge (l_s):

$$S = \frac{l_e}{l_s} \tag{1}$$

Sinuosity is important because it is related to the discharge within the channel (cf. Makaske, 2001) and to the width−depth ratio and sediment load of the channel (cf. Schumm, 1963). Moreover, sinuosity is a required parameter for models and tracer experiments in subglacial channels (e.g. Schuler and Fischer, 2009). Eskers are often described as sinuous (e.g. Clark and Walder, 1994; Syverson et al., 1994; Warren and Ashley, 1994), although there are few reports or quantification of esker sinuosity. Bolduc (1992) measured the sinuosity of esker ridges in Labrador and found that sinuosity varied between 1.00 and 1.32. A recent study of the Chasm esker, British Columbia, Canada (Burke et al., 2012) noted a sinuosity value of 1.07. Our extraction of sinuosity values for the esker ridges mapped in the UK and Kola Peninsula by Clark et al. (2004) and Hättestrand and Clark (2006) indicate a mean esker ridge sinuosity of 1.03 and 1.06, respectively (Fig. 3B).
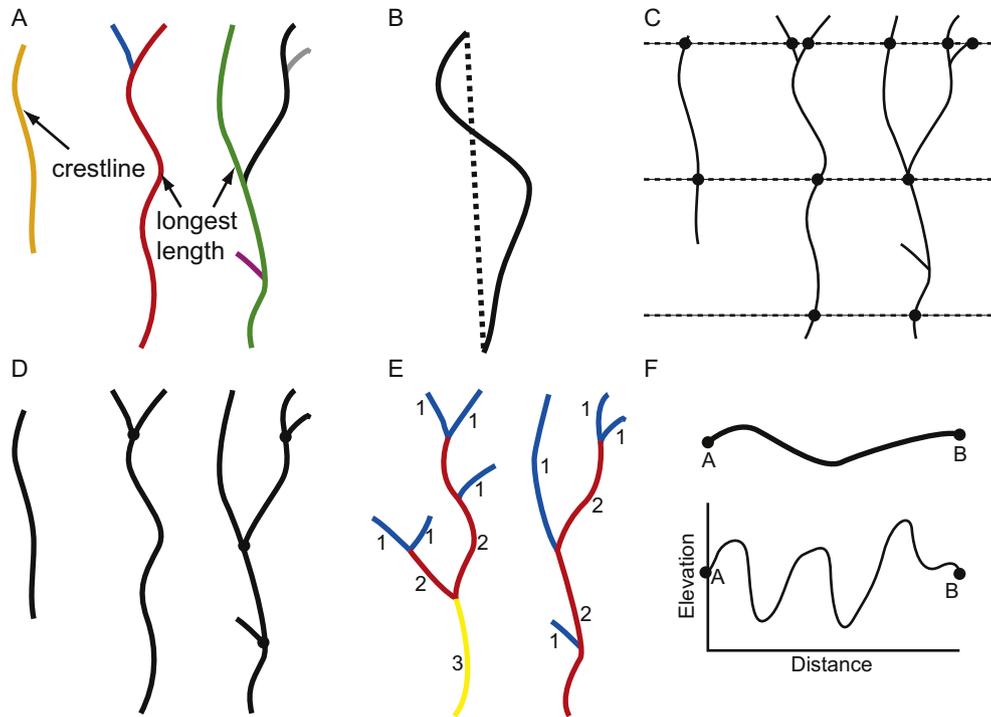
Fig. 1. The different methods used to calculate the six parameters in this paper. A) Length: each shaded colour represents possible length measurements. Where tributaries coalesce, the longest measurement was extracted. B) Sinuosity: the length of the esker ridge was divided by the length of a straight line between the start and end points. C) Lateral spacing was calculated by measuring the distance between points produced where eskers intersect equidistant parallel transects, the locations of which are indicated by the black boxes in Fig. 5. Esker density was calculated by producing points where eskers intersect published ice margins and intermediate, interpolated ice margins. It is expressed as the number of eskers per 100 km of ice sheet margin (see text for description). D) Tributaries: points were created where two or more esker ridges intersect and the number of intersections was calculated between two margin time steps. E) Stream ordering: the Strahler number for each esker was calculated manually, based on the number and order of tributaries entering each esker. F) Elevation change: elevation values were extracted at the beginning and end points of each esker from the Canadian Digital Elevation Database (CDED) to assess whether eskers trend up- or down-slope. (For interpretation of the references to colour in this figure legend, the reader is referred to the web version of this article.)
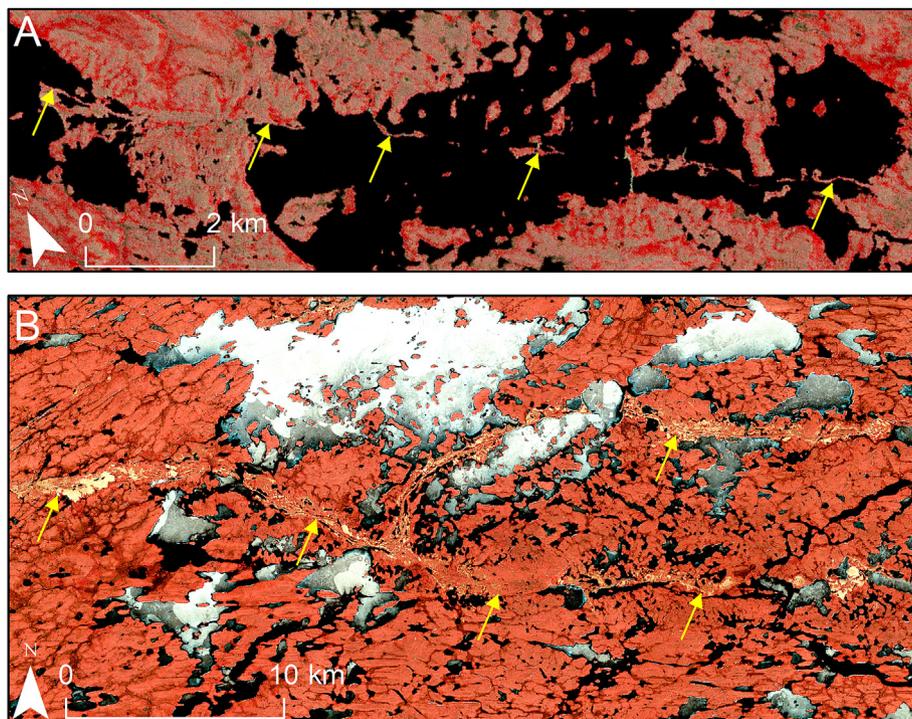

Fig. 2. Examples of Canadian eskers in pan-sharpened Landsat 7 ETM+ imagery (R, G, B = 4, 3, 2). A) A straight, heavily fragmented esker in Labrador. B) Tributary and trunk eskers in Northwest Territories.
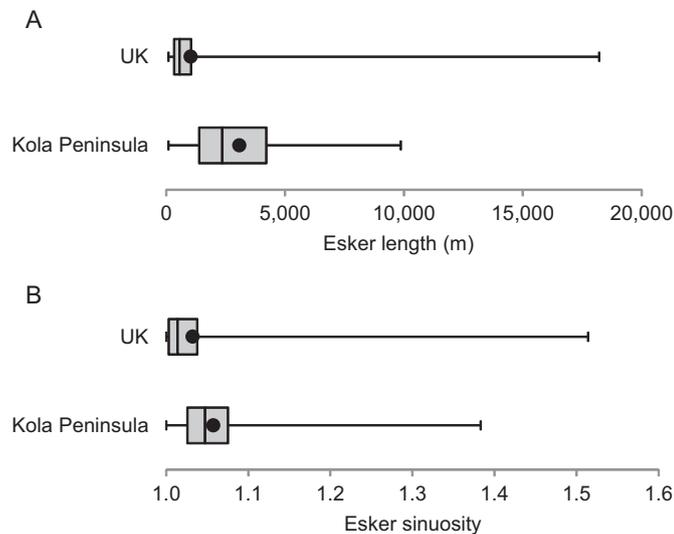
Fig. 3. Box and whisker diagrams showing A) esker ridge length data and B) esker ridge sinuosity data for the UK ($n = 857$) and Kola Peninsula, Russia ($n = 817$). Whiskers denote the range of values, points denote means and the boxes span the range of the 25—75% percentiles, with the median as a vertical bar. Data were extracted from shapefiles published in Clark et al. (2004) and Hättestrand and Clark (2006).

2.4. Lateral spacing of eskers

Esker spacing refers to the lateral distance (transverse to ice-flow) between adjacent eskers (including both trunk and tributary eskers; Fig. 1C). Numerical models have been developed which predict the spacing between eskers as a product of the interaction between subglacial meltwater in conduits and groundwater in permeable substrata (Boulton et al., 2007a, b; Boulton et al., 2009), or in a surrounding distributed system (Hewitt, 2011; Werder et al., 2013). Several papers have reported measurements or model predictions of the spacing of eskers or subglacial channels, summarised in Fig. 4. The values vary between 2 and 35 km, but the values reported for different parts of the LIS appear to indicate a preferred spacing of 12—15 km (Banerjee and McDonald, 1975; St-Onge, 1984; Shilts et al., 1987; Bolduc, 1992). To date, the only application of spacing measurements to test numerical modelling is provided by Boulton et al. (2009) who noted that esker spacing, which they measured to between 2.5 and 33 km, was generally consistent with their modelled channel predictions for a study area in Finland.

2.5. Tributaries and stream ordering

It has long been observed that esker systems often consist of trunk and tributary eskers (e.g. Fig. 2B; Flint, 1928; Price, 1966; Aylsworth and Shilts, 1989a; Brennand, 1994; Clark and Walder, 1994), probably reflecting the hydrological network in which they were formed, and the former ice surface topography, which exerts some control on their development. Thus, the number and order of tributaries may provide an insight into the connectivity of the drainage system. Mapping tributaries joining trunk eskers may thus allow an estimate of the extent and efficiency of former sub-glacial meltwater drainage systems, although it should be noted that eskers may form only one component of the drainage system and that other parts (e.g. supraglacial channels) may go unrecorded. Few data have been presented on esker tributaries, but Banerjee and McDonald (1975) noted that esker systems very rarely contain more than two orders of tributaries. Conversely, Aylsworth and Shilts (1989a) noted that esker systems in the Keewatin sector of the LIS contain up to fourth-order tributaries.

2.6. Topography/slope

Theoretically, eskers will follow the hydraulic gradient, which is determined by the ice surface slope and bed topography (Shreve, 1972), implying that they can sometimes climb 'uphill'. Eskers have been observed to climb upslope by many authors (e.g. Sissons, 1958; Price, 1969; Shreve, 1985a; Brennand, 1994), though whether this is typical is yet to be investigated because there has been no systematic analysis of large sample sizes.

3. Methods

3.1. Datasets

We analyse esker morphometry and pattern from two datasets. The first is an ice sheet-wide map of 20,186 large (mostly > 2 km long) esker ridges digitised from Landsat 7 ETM+ imagery of Canada, recently published as a map in Storrar et al. (2013). Esker ridge crestlines were digitised directly into a Geographic Information System (GIS) and were stored as polyline shapefiles (see Fig. 5). Typically, red, green, blue band combinations of 4, 3, 2 or 7, 5, 2 were used to identify eskers, which were then mapped at scales of approximately 1:40,000.

Spatial variation in vegetation characteristics (e.g. forest cover) and agricultural development mean that eskers are typically more difficult to detect in southern Canada, and more readily detectable
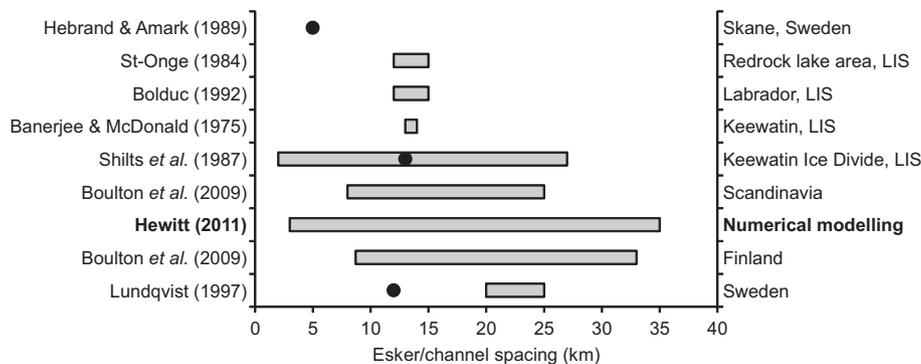

Fig. 4. Examples of esker/subglacial channel spacing quoted in the literature. Bars represent stated maxima and minima and points represent stated means. Bold fonts indicate numerical model outputs and regular fonts indicate observations. LIS = Laurentide Ice Sheet. Note that the mean value quoted by Lundqvist (1997) includes what they term 'minor' esker ridges, whereas the quoted range relates to their 'major' eskers only.
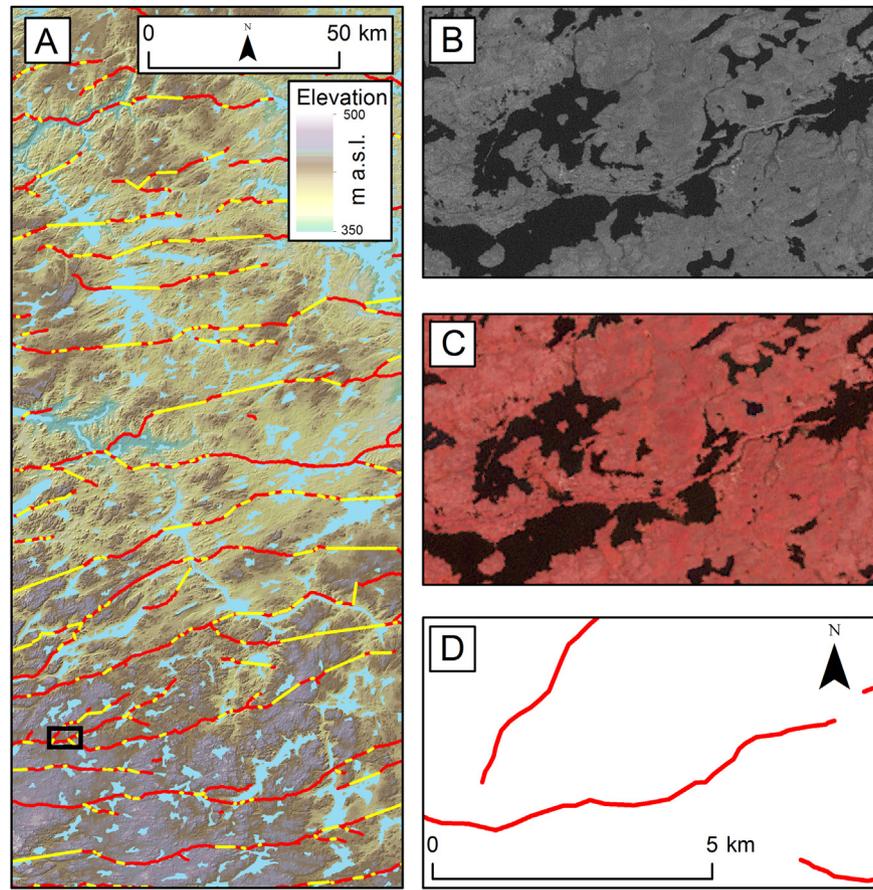
Fig. 5. A) Example of digitised esker ridges (red) and 'interpolated' eskers (yellow), which join breaks in esker ridges. Location of B, C and D is shown by the black box. Elevation data are from the Canadian Digital Elevation Database. B) Eskers in band 8 of a Landsat 7 ETM+ image; C) Eskers in a false colour composite (R, G, B = 4, 3, 2) Landsat image; D) Eskers digitised from B) and C). Note fragmentary nature of esker ridges, mostly due to lakes. (For interpretation of the references to colour in this figure legend, the reader is referred to the web version of this article.)

in the north (see Storrar et al., 2013). By coincidence, this means that eskers associated with the deglaciation of the former Keewatin and Labrador domes of the LIS are more easily detected than eskers which formed earlier (e.g. under the southern lobes of the LIS). Consequently, we focus primarily on the eskers associated with the Keewatin and Labrador sectors during the later stages of deglaciation of the LIS.

Another potential drawback when mapping from Landsat imagery is that the spatial resolution (30 m and 15 m in the panchromatic band), is likely to prevent some very small esker ridges from being detected. As a cross-check of the mapping, seven areas (see Fig. 6), covering roughly 175,000 km^2, were also mapped by Storrar et al. (2013) from high resolution aerial photography. It was found that approximately 75% of esker ridges were detected in Landsat imagery, with 81% of the undetected esker ridges being <2 km long (Storrar et al., 2013). Thus, whilst we acknowledge that some small esker ridges are missing from our data, we do not consider this a major limitation because the emphasis here is on large-scale patterns and measurements of the largest conduits.

For further analysis of some metrics, such as the maximum length of eskers and lateral spacing, we also derived a second dataset whereby 'gaps' between mapped esker ridges (that result from fragmentary deposition, post-depositional erosion or submergence beneath lakes) were filled by interpolating a straight line between aligned esker ridges which appeared to be genetically related (i.e. not separated by excessively long gaps in comparison to

the ridges themselves). The gaps were then merged with the mapped esker ridges, thereby providing a single esker the full length of the series of subset ridges. This dataset was produced in order to avoid statistics that would be distorted by the absence of esker ridges for the above reasons. Some measurements, such as the spacing between subglacial channels, are overestimated if there are gaps in eskers; conversely, the length of subglacial channels is underestimated (assuming that the gap was previously occupied by a channel that did not subsequently form an esker). Thus, the 'interpolated' dataset indicates where the major channels which formed the eskers were generated. Esker ridges were joined conservatively (13,314 'gaps' were connected, of which 94% were <10 km long) and the fact that the gaps are relatively small, in comparison with the surrounding longer esker ridges (sometimes 10s of km long), gives us confidence that they connect eskers which are genetically related (see Fig. 5A). We refer to the two datasets as *mapped* and *interpolated* eskers, respectively.

3.2. Measurements

3.2.1. Length (l_e)

Esker crestline lengths were extracted from the *mapped* and *interpolated* data, to allow an estimation of the fragmentation of eskers and also to provide an approximate measurement of the maximum length of the esker-forming conduit. Where two or more eskers coalesced, the longest ridge was systematically used to determine length (see Fig. 1A).
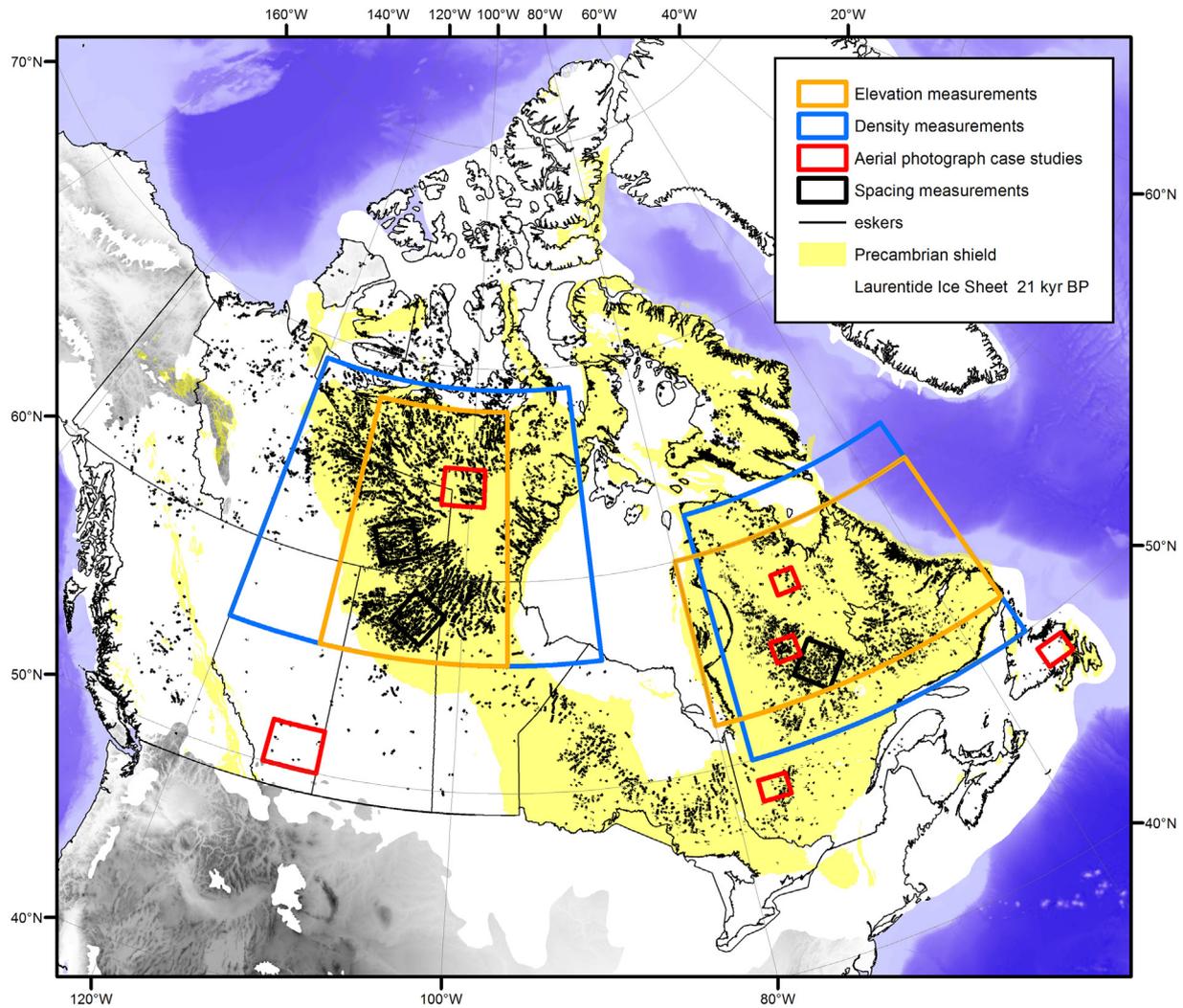
Fig. 6. Esker ridges mapped from Landsat imagery of Canada (black). Also shown are the areas mapped by aerial photography, used to check the consistency of the Landsat images; the areas used to calculate spacing and density in the Keewatin (west) and Labrador (east) sectors; the areas used to calculate esker spacing in high density locations (see section 3.2.3); and the areas used to measure elevation changes. The Precambrian Shield is shown in yellow (from Wheeler et al., 1996). (For interpretation of the references to colour in this figure legend, the reader is referred to the web version of this article.)

3.2.2. Sinuosity(S)

Sinuosity was calculated using equation (1), for both *mapped* and *interpolated* eskers using l_e and the length of a straight line (l_s) between the co-ordinates of the esker start (x_{start} and y_{start}) and end (x_{end} and y_{end}) points:

$$l_s = \sqrt{(x_{end} - x_{start})^2 + (y_{end} - y_{start})^2} \qquad (2)$$

Measurements of esker sinuosity are sensitive to the length of the esker: very short eskers tend to have very low sinuosity values because they often make up short, straight segments of a larger, more sinuous system (see Fig. 7A). Thus, because the *mapped* eskers represent a fragmented view of the channels in which they formed, it is likely that the sinuosity values calculated from them are an underestimate of the sinuosity of the original channels in which they formed.

In order to explore this potential bias, we conducted a sensitivity analysis, whereby the *mapped* eskers were used to test the extent to which calculations of sinuosity are distorted by the length of the esker ridge. We deliberately split the *mapped* eskers into smaller ridges of different lengths (in 0.5 km increments from 0.5 km to

20 km: see Fig. 7 for details) and measured the sinuosity of all the smaller ridges in each case. The results are shown in Fig. 7, which confirms that longer fragments of eskers tend to have higher sinuosity values. The relationship is well represented by a power law ($S = l_e^{0.015}$ for median sinuosity [$R^2 = 0.99$]; $S = l_e^{0.016}$ for mean sinuosity [$R^2 = 0.99$]). The mean and median sinuosity values of the *mapped* esker dataset lie within the upper and lower values obtained from this analysis (dashed lines in Fig. 7C) and give us confidence that although they are likely underestimates, the magnitude of this error is on the order of ~0.05, which is relatively small.

3.2.3. Lateral spacing

In order to examine esker spacing and test model predictions of this characteristic, it is helpful to measure the spacing between eskers in an area where they are sufficiently dense to represent the majority of the channels in which they were formed (models do not generally account for the non-formation or subsequent erosion of eskers, as would be the case for an entire ice sheet bed). Three large (40,000 km^2) sample areas (see Fig. 6) were selected where eskers are numerous and appear to be well preserved, with minimal evidence of postglacial erosion. Each area was divided into
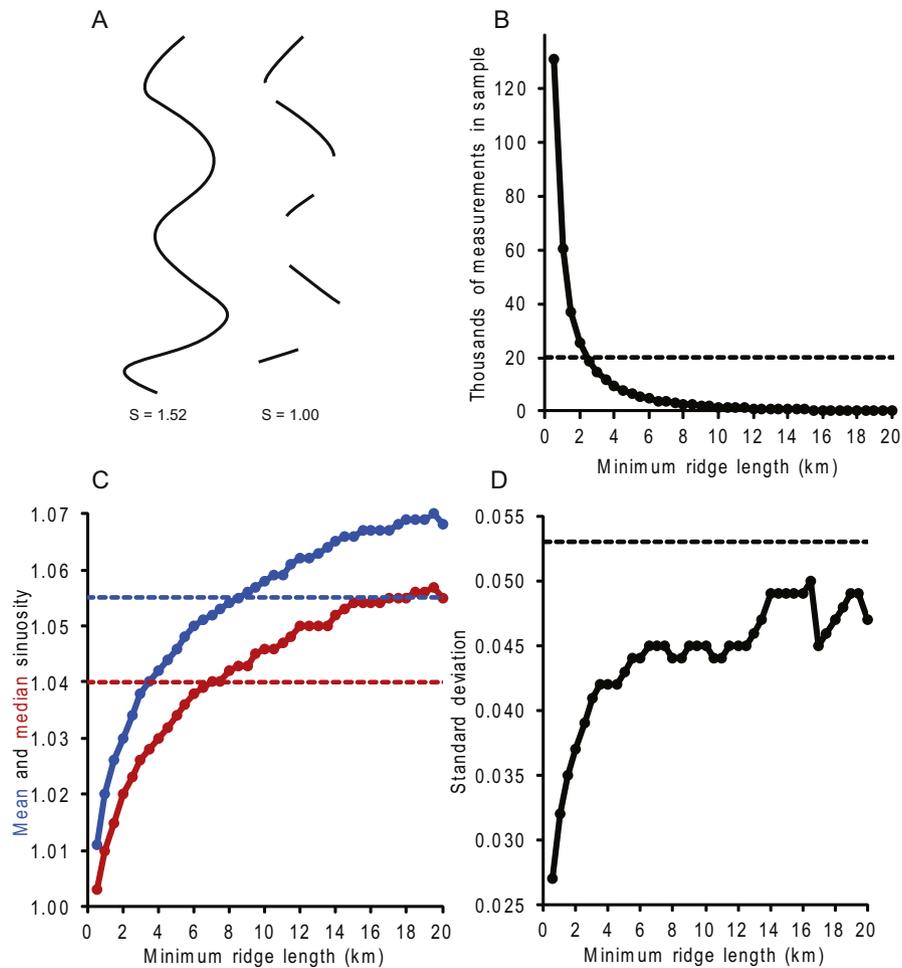
Fig. 7. The effect of esker length on sinuosity measurements. A) Illustration of how sinuosity increases with ridge length. The sinuosity of the long ridge on the left is 1.52, whereas the mean sinuosity of the smaller subsets on the right is 1.00. B–D) An experiment to determine the effect of esker length on the sinuosity measurements of 20,186 *mapped* eskers. The *mapped* eskers were split into portions of equal length and the sinuosity of each portion measured. This was repeated for different lengths, in 0.5 km intervals between 0.5 and 20 km, resulting in 40 different datasets, with more measurements possible for shorter sample lengths and fewer for larger lengths (B). Mean and median (C) and standard deviation (D) values were then derived from each dataset. The dashed lines in B–D indicate the value calculated from the entire, unaltered *mapped* eskers dataset.

15×200 km transects aligned perpendicular to the dominant esker orientation and spaced 12.5 km apart. Esker spacing was calculated along each transect, for both *mapped* and *interpolated* eskers (Fig. 1C).

3.2.4. Esker density during deglaciation

Changes in esker density (the number of eskers per 100 km of ice sheet margin) through deglaciation, from 13 to 7 ka BP, were calculated in two large study areas, corresponding to the eskers which formed beneath the Keewatin and Labrador sectors of the ice sheet (see Fig. 6; Storrar et al., 2014). Esker density was calculated where they intersected with the former ice margin positions of the LIS, as depicted in the chronology of Dyke et al. (2003). The chronology is based on approximately 4000 minimum-limiting dates, primarily from radiocarbon dating, which carry an associated uncertainty, conservatively estimated at ±500 years (see Dyke et al., 2003 for further details). Areas where lakes, rivers and oceans coincided with the margin were not used in the measurements. In places, we also interpolated intermediate margins to increase the sample size. This was done by visually interpolating margins between adjacent margins. Error bars are included in all graphs which indicate the two dated margins between which the intermediate margins were interpolated. Ice sheet retreat rate was calculated from 20 transects across the Dyke et al. (2003) margins in each area.

The results of the analysis of *mapped* eskers are presented in Storrar et al. (2014), which we discuss here in relation to the *interpolated* eskers.

3.2.5. Tributaries

The numbers of tributaries in esker systems were extracted from the GIS (Fig. 1D). As a result of the fragmentary nature of the eskers, relatively few tributaries are connected to a trunk esker in the *mapped* esker data. Thus, tributaries were also calculated for the *interpolated* eskers, which are likely to be more representative of situations where two esker-forming conduits were confluent. In order to explore whether the proportion of tributaries in esker systems evolves through time, the number of tributaries per 100 km of the length of *mapped/interpolated* eskers was calculated for seven time slices. The time slices were based on the margin positions of Dyke et al. (2003). Eskers were also numbered according to the Strahler method of stream ordering (Fig. 1E). During the generation of the *interpolated* eskers, some tributary eskers were connected to trunk eskers where they were in close proximity and appeared to be converging. This could potentially bias stream order calculations if these situations do not reflect former tributaries. Thus, we present data for both *mapped* and *interpolated* eskers in Section 4.6.

3.2.6. Topography/slope

The difference in elevation between the start and end points was calculated for 11,560 *mapped* esker ridges in the Keewatin and Labrador sectors (Fig. 6). The locations selected for the analysis contain a large sample of esker ridges within an area in which we are confident that flow was away from the final locations of the ice domes (Shilts et al., 1987; Aylsworth and Shilts, 1989a; Clark et al., 2000). We refrain from analysing the entire dataset because esker ridge orientation, with relation to ice movement, is not always known, especially where their plan form is more chaotic. Elevations were taken from the Canadian Digital Elevation Database (CDED), which has a horizontal resolution of approximately 20 m and vertical resolution of 1 m. Elevation changes were determined by subtracting the elevation at the end point of each esker ridge from the elevation at the start point. This value was then used alongside the length data presented in Section 3.2.1 to calculate the overall slope of each esker ridge, with negative values denoting a decrease in elevation down-ice and positive values reflecting an increase in elevation down-ice. The measurements relate to the elevation of the topography at the points at which esker ridges initiate and terminate, and so reflect the extent to which esker ridges trend up- or down-slope, rather than any changes in the height of the actual landform.

4. Results

4.1. Pattern and distribution

A total of 20,186 large esker ridges were analysed (Fig. 6; Storrar et al., 2013) and, most obviously, the majority of large esker ridges (84% of esker ridges > 10 km long) are concentrated on the Canadian Shield, as noted by Clark and Walder (1994). Nevertheless, eskers are also present in other areas, where potentially more deformable substrates, rather than resistant shield rocks, predominate, and indicating that channelised drainage can occur over softer sedimentary beds (cf. Shoemaker, 1986; Mooers, 1989). The distribution of eskers over the Thelon and Athabasca sedimentary basins, which form part of the Precambrian shield but are more readily erodible than typical shield rocks (e.g. the Slave craton), is shown in Fig. 8.

At the largest scale, eskers are seen to form a radial pattern around the final positions of the ice divides in Labrador and Keewatin (Fig. 6; Dyke and Prest, 1987; Aylsworth and Shilts, 1989a, 1989b; Boulton and Clark, 1990), beneath which they are noticeably absent: esker-free areas are roughly 100–150 km wide in both Keewatin and Labrador and cover an area of approximately 93,000 and 174,000 km^2, respectively (Fig. 6). Within the radial systems, regularly spaced channels appear to correspond to an integrated system of eskers with multiple tributaries (e.g. Fig. 9B). Outside of the systems, esker patterns are more chaotic, with some branching esker systems, but with many discrete single eskers or areas of eskers which appear to be unrelated (e.g. Fig. 9C and D).

4.2. Length and fragmentation

The length of *mapped* esker ridges follows a log-normal distribution (Fig. 10), with a skewness of 4.57 and excess kurtosis of 40.94. Individual esker ridges extend up to 97.5 km, with a mean of 3.5 km and median of 2.1 km. 56% of esker ridges are 1–5 km long and 70% are 1–10 km long.

When gaps are taken into account, *interpolated* eskers extend for up to 760 km and have a mean length of 15.6 km and median of 4.1 km. Assuming that most gaps have been correctly identified (of which we are confident: see Fig. 5), this shows that eskers are highly fragmented within the channels in which they formed. Gaps

represent 34.9% of the total length of the *interpolated* eskers. The distribution is also approximately log-normal, with skewness of 6.57 and excess kurtosis of 71.61. Figs. 11 and 12 reveal that the longest and least fragmented esker systems are associated with the Keewatin sector of the LIS. There are also eskers up to 290 km long in Quebec, associated with the Labrador dome, but they are significantly more fragmented than those of Keewatin. No discernible trends in fragmentation are apparent along the *interpolated* eskers (Fig. 12B).

4.3. Sinuosity

Mapped esker ridge sinuosity follows a distribution similar to log-normal, although it is more positively skewed (skewness = 3.41) towards lower values. Indeed, 87% of esker ridges have a sinuosity value between 1.00 and 1.10, and 98% have a sinuosity value of between 1.00 and 1.20. The mean value is 1.06 and the median is 1.04. *Interpolated* esker sinuosity has a similar distribution but values tend to be slightly higher (as expected: see Section 3.2.2), with a mean of 1.08 and median of 1.06 (Fig. 13).

4.4. Lateral spacing

Measurements of esker spacing in three sample areas indicate that the distribution of spacing data follow a more normal distribution (Fig. 14) than length and sinuosity. *Mapped* esker ridges have a higher mean spacing than *interpolated* eskers (18.8 km compared with 12.3 km), as would be expected because fewer *mapped* esker ridges intersect transects, compared with the more continuous *interpolated* eskers. Likewise, standard deviation values of esker spacing are higher for the *mapped* esker ridges than the *interpolated* eskers. The three sample areas, when treated individually, produce broadly similar results for esker spacing (see Table 1). The *mapped* esker mean data values vary by 3.7 km and the *interpolated* esker mean data vary by just 0.3 km. Mean esker spacing in the three areas when combined is 18.8 km (standard deviation is 14.0 km) for *mapped* eskers and 12.3 km (standard deviation is 6.6 km) for *interpolated* eskers. The relatively low standard deviations, compared with the means, suggest that esker spacing is approximately regular, particularly in the case of the *interpolated* eskers.

4.5. Esker density during deglaciation

Data on the density (number of esker ridges per 100 km of ice margin) of the *mapped* eskers during deglaciation were discussed in Storrar et al. (2014). In the present paper, we show data for both *mapped* eskers and *interpolated* eskers, demonstrating that they reveal similar patterns. Thus, data for *interpolated* eskers appear in brackets, after the equivalent values for *mapped* eskers, in both Sections 4.5 and 4.6.

In the Keewatin sector, esker density increased from 0.7 (1.1) to 3.0 (4.4) eskers per 100 km of ice margin from 13 to 9 ka BP (Figs. 15 and 16). Between 9 and 8.5 ka BP, esker density abruptly decreased from 3.0 (4.4) to 0.8 (1.2) eskers per 100 km of ice margin. Following 8.5 ka BP, the decrease in esker density was more gradual. The retreat rate of the ice sheet in this sector was between 100 and 200 m yr^{-1} from 13 to 9.5 ka BP, but increased rapidly to 397 m yr^{-1} from 9.5 to 9 ka BP, before decreasing sharply between 8.5 and 8 ka BP (Fig. 16).

Data from the Labrador sector reveal a slightly different pattern. Esker density was less than 0.8 (1.1) eskers per 100 km of ice margin between 13 and 8 ka BP and then increased to 1.8 (3.2) by 7.6 ka BP, decreasing thereafter until no further eskers formed after approximately 6.5 ka BP. The ice sheet retreat rate was between 30 and
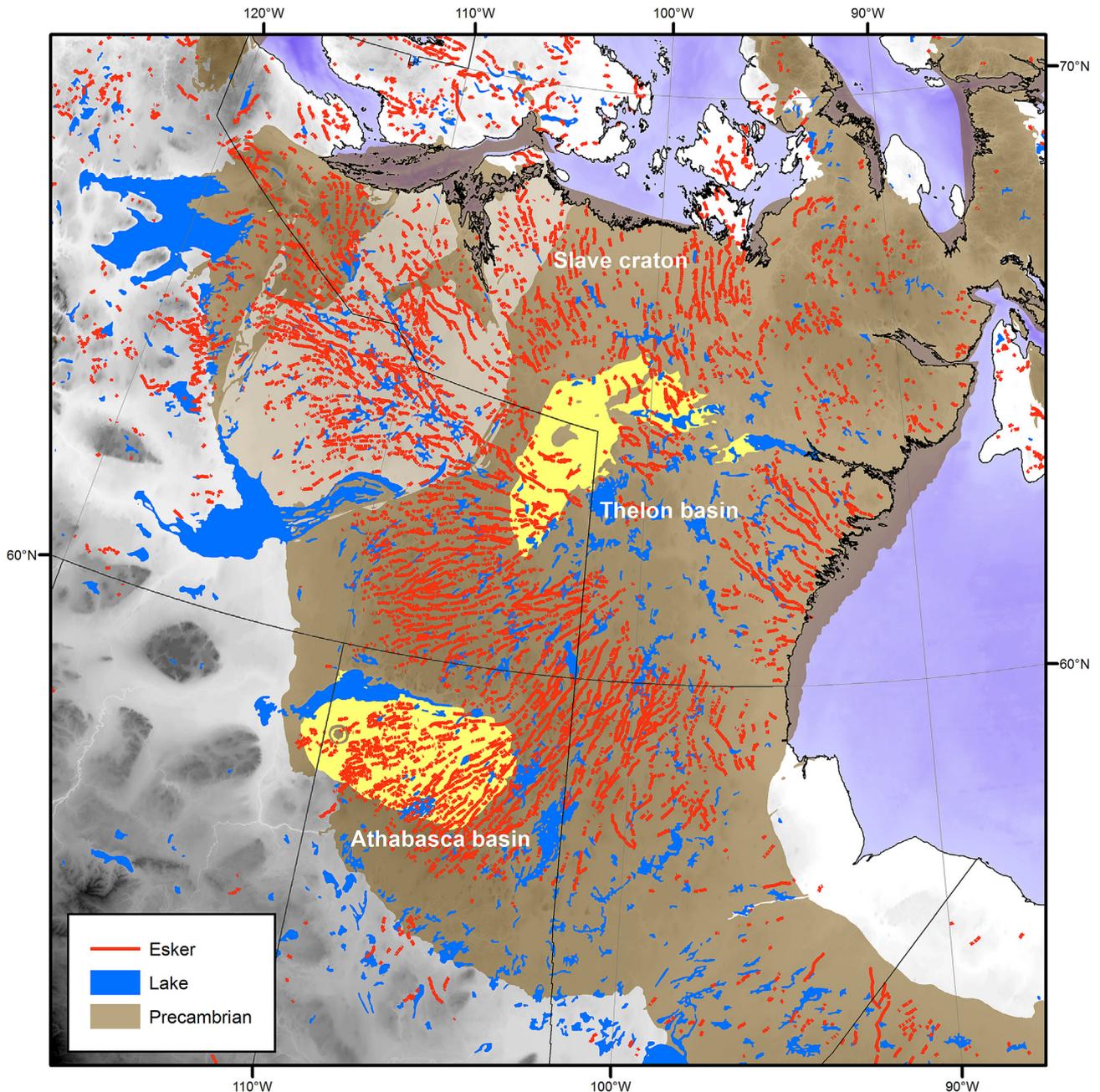
Fig. 8. Esker distribution in relation to the Precambrian Shield, including the Slave craton and Athabasca and Thelon sedimentary basins (after Wheeler et al., 1996), in the Keewatin sector of the LIS.

60 m yr^{-1} from 13 to 8.6 ka BP and then increased to 150 m yr^{-1} by 7 ka BP (Fig. 16).

4.6. Tributaries

Overall, 475 (1335 *interpolated*) tributaries were identified for the *mapped* eskers, which equates to 0.67 (1.22) tributaries per 100 km of total esker length. The number of tributaries per 100 km of esker length decreased from 25.8 (91.0) to 0.1 (0.1) between ~13 and ~7 ka BP in the Keewatin sector. In the Labrador sector, the number of tributaries per 100 km of esker length decreased overall between ~11.4 ka BP and ~7 ka BP from 1.9 (2.4) to 0 (0.2), but with a small peak at ~7.5 ka BP.

The extensive fragmentation of the *mapped* eskers resulted in the identification of few tributaries. Thus, the majority (96.5%) of eskers were found to be first-order, with 3.5% second-order tributaries and only two third-order (Table 2). Analysis of tributary ordering using *interpolated* eskers reveals, unsurprisingly, a much more integrated pattern. *Interpolated* esker systems possess more tributaries, especially around the Keewatin sector (Fig. 17). Fourth-order eskers are noted in two locations and second-to fourth-order eskers account for approximately 25% of all the *interpolated* eskers (Table 2).

4.7. Topography/slope

Within the areas where slope was analysed, the majority (97.5%) of eskers occur on terrain with an elevation of <700 m a.s.l., and 60% are located between 300 m a.s.l. and 600 m a.s.l. The mean value is 344 m a.s.l. (Fig. 18C). Visual
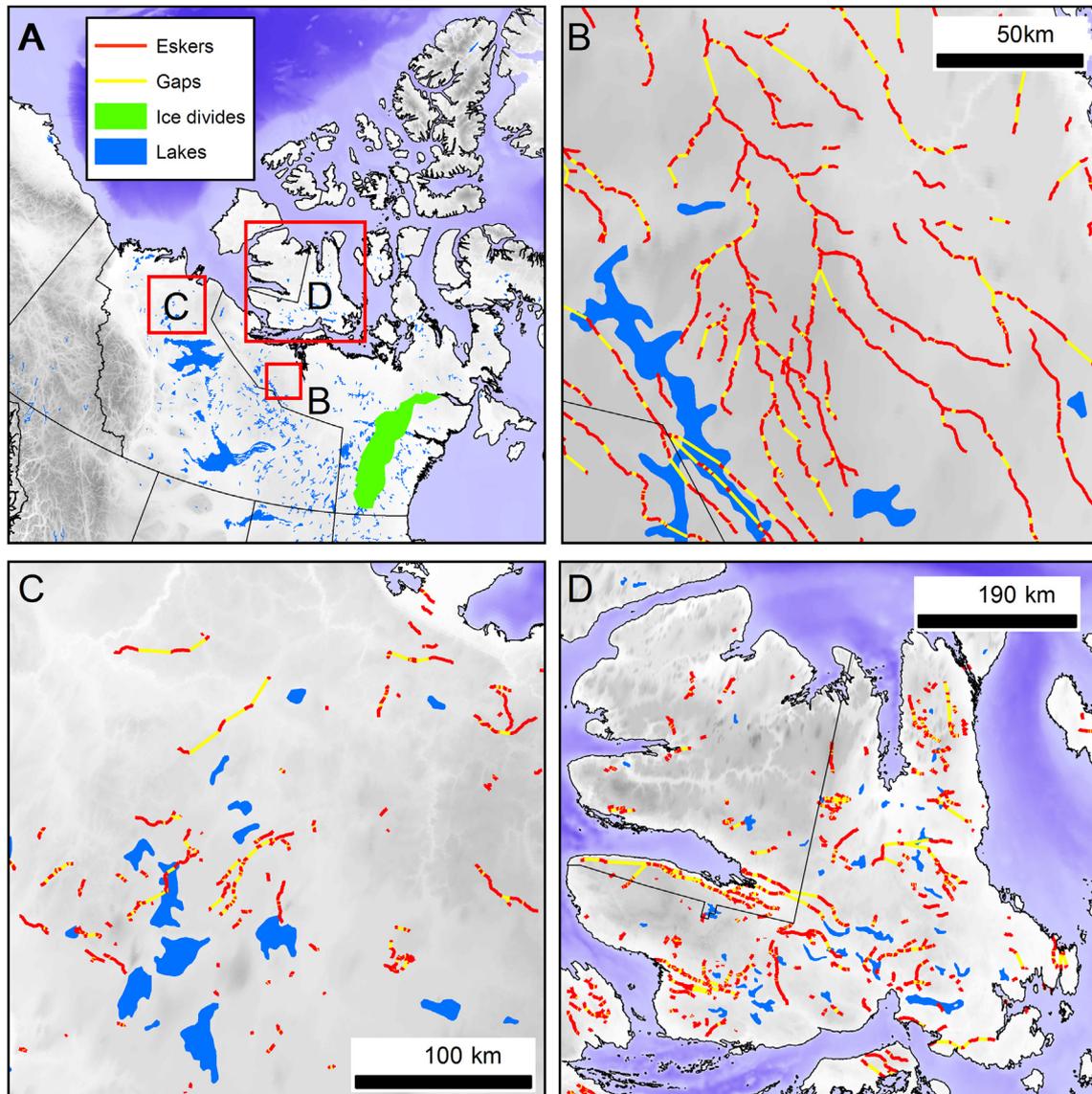
Fig. 9. Esker patterns. B) Integrated dendritic network with multiple tributaries, typical of the esker systems in the Keewatin sector (location shown on A). C) and D) Chaotically arranged eskers typical of the Canadian Arctic and far north-west.

comparison of *mapped* esker locations with topographic data suggests that, whilst some esker ridges tend to follow the thalwegs of valleys, and some eskers in the Keewatin region appear to terminate at the end of plateaux, the overall distribution of esker ridges is not strongly related to variations in topography (Fig. 19).

Mapped eskers predominantly exhibit small changes in elevation (small slopes) along their length (Fig. 18). The mean change in absolute elevation for 11,562 eskers is just +1.04 m, implying a small increase in elevation down-ice (which corresponds to a mean slope of 0.02°). 73% of the eskers change in elevation by no more than ±10 m. The absolute elevation change values are normally distributed about 0 m, and the mean slope values are normally distributed about 0.1°, indicating that there is no clear uphill or downhill trend to esker profiles, although the largest elevation change is in the downslope direction (−160 m). 4636 (40%) eskers trend downhill, 1864 (16%) exhibit no change in elevation and 5062 (44%) trend uphill (by up to 143 m).

5. Discussion

5.1. Pattern and distribution

Although our dataset is much larger than the one presented in Clark and Walder (1994), large scale observations of the relative abundance of eskers on the Canadian Shield, compared with other areas where eskers are rarer, shorter and more fragmented, supports their hypothesis that eskers form preferentially over more resistant substrates. They argued that this is because subglacial meltwater channels would be more likely to be incised upwards into the ice over the crystalline bedrock. Note, however, that eskers have also been mapped, albeit in smaller numbers, in areas of deformable substrate off the Canadian Shield (see Fig. 6) as well as in parts of the northern USA (e.g. Wright, 1973; Mooers, 1989). Moreover, it is likely that the mapping from satellite imagery has missed a number of small eskers over these areas (Storrar et al., 2013). In summary, whilst the hypothesis of Clark and Walder
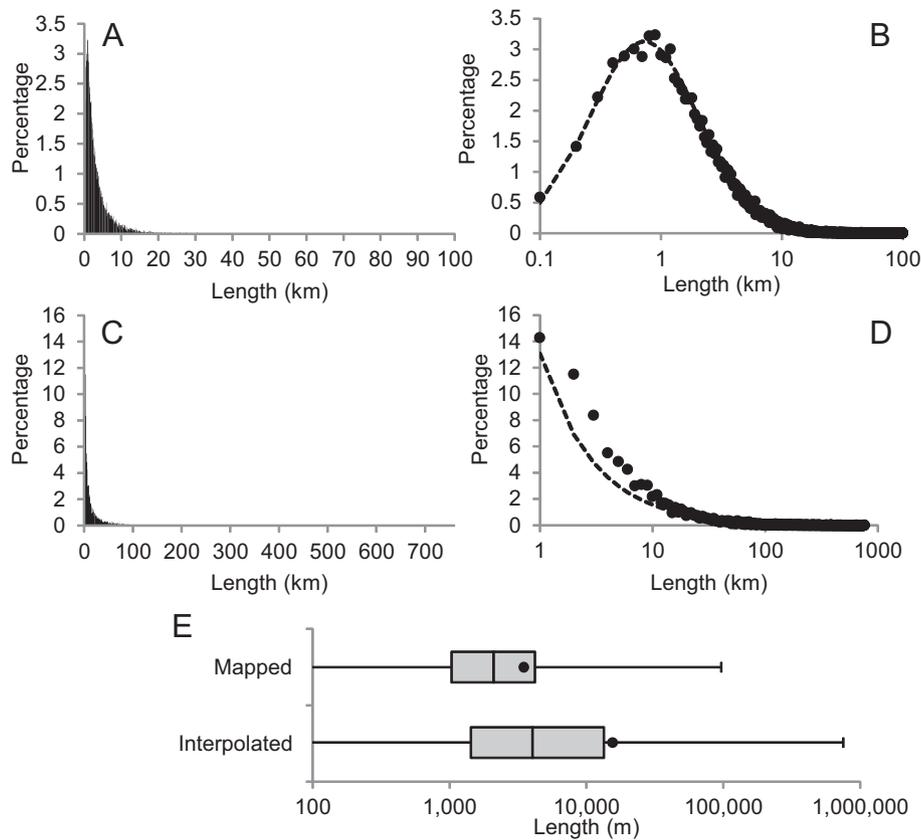
Fig. 10. Esker length statistics. A) Histogram of *mapped* esker ridge length ($n = 20{,}186$, 1 km bins). B) *Mapped* esker ridge length plotted on $\log_{10}$ x-axis (1 km bins). A log-normal distribution with the same mean and standard deviation is shown by the dashed line. C) Histogram of *interpolated* esker length ($n = 5{,}932$, 1 km bins). D) *Interpolated* esker length plotted on $\log_{10}$ x-axis (1 km bins). A log-normal distribution with the same mean and standard deviation is shown by the dashed line. E) Box and whisker plot comparing *mapped* and *interpolated* esker length measurements. Whiskers denote the range of values, points denote means and the boxes span the range of the 25–75% percentiles, with the median as a vertical bar. Note the $\log_{10}$ x-axis.

(1994) may be able to account for the gross distribution of eskers, there are some exceptions which their hypothesis cannot explain, and for which we now provide some alternative explanations.

Importantly, whilst the large esker systems in Canada are strongly coincident with the Precambrian rocks of the Canadian Shield, they are also coincident with the locations of the former Keewatin and Labrador domes during the later stages of deglaciation. Significant changes in the depositional environment during deglaciation, including the transition from being largely marine-terminating to terrestrially-terminating (see Dyke et al., 2003), as well as changes in the supply of meltwater (e.g. Carlson et al., 2009), mean that lithology cannot be isolated as a single control on esker distribution and the spatial coincidence of these two potential controls makes them difficult to separate. The influx of meltwater during deglaciation has been linked to increases in esker density, which points to a climatically driven meltwater supply control on esker distribution (Storrar et al., 2014). This is not incompatible with eskers *also* forming preferentially on certain lithologies and it appears likely that variable meltwater fluxes and lithology have exerted some control on the observed esker pattern. The preferential occurrence and spacing of eskers over different lithologies has been related to substrate permeability, rather than deformability (e.g. Grasby and Chen, 2005; Boulton et al., 2009), which explains how eskers can be related to particular geological units and also exist over deformable substrates. It is also worth noting that eskers are prevalent over the Athabasca sedimentary basin and parts of the Thelon sedimentary basin, which are both on the Precambrian Shield (Fig. 8). These basins are composed of relatively erodible sandstones (Wheeler et al., 1996) and it is likely that they provided a significant source of sediment to build eskers, and may present an additional explanation for esker distribution on the Shield (e.g. Shilts et al., 1987; Aylsworth and Shilts, 1989a). Parts of the Thelon basin are relatively devoid of eskers, which may be related to distributed (rather than channelised) meltwater drainage associated with the Dubawnt Lake Palaeo-ice stream (Stokes and Clark, 2003a, b), rather than sediment supply.

Outside the areas formerly occupied by major ice divides, esker systems are arranged in integrated radial networks of up to fourth-order tributaries, reflecting the network of conduits in which the eskers formed and supporting the observations of Shilts et al. (1987). The continuous retreat with few readvances of the ice sheet in these areas (Dyke et al., 2003) made it possible for this integrated pattern of eskers to be preserved. In other locations, notably western Northwest Territories and Victoria Island, esker ridges are distributed more chaotically (Fig. 9). It is likely that this reflects the deposition of esker ridges during different phases of rapidly-changing flow trajectories which operated in these areas as ice streams switched on and off (Kleman and Glasser, 2007; Stokes et al., 2009; Brown et al., 2011). The regions supporting these more 'disorganised' eskers exhibit greater variability in topography than the Shield areas (see Fig. 19). It may be the case, therefore, that the complex ice dynamics associated with these areas, which resulted in the more chaotic esker patterns is, in part, related to topographic variability. A low-profile ice sheet interacting with variable
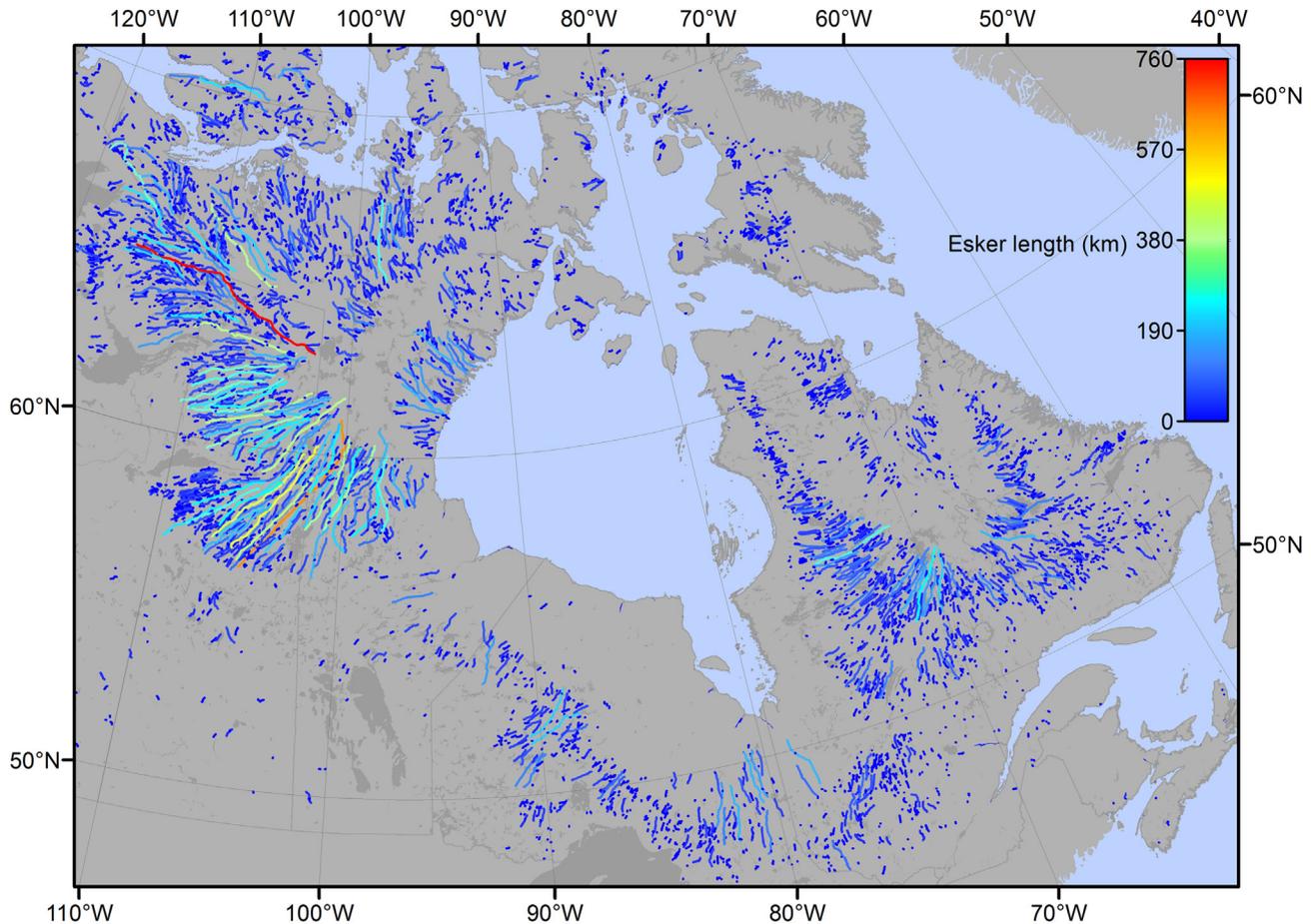
Fig. 11. Map of *interpolated* eskers classified by length. Note the radial pattern of long eskers around the Keewatin (west) and Labrador (east) sectors.

topography is likely to experience more change than a similar ice sheet flowing over more homogeneous terrain.

Within Shield areas, there are also places where eskers are noticeably absent, particularly in the locations of the Keewatin and Labrador ice domes (Fig. 6). Evidently, this is not related to the underlying geology, but rather ice and meltwater dynamics. Meltwater channels are unlikely to form beneath ice divides because any meltwater there would need to accumulate for a certain distance before it was able to form channels (e.g. Flowers et al., 2003). Furthermore, the ice is likely to have been cold-based until the final stages of deglaciation (Kleman and Glasser, 2007), thus routing surface-generated meltwater over and across the ice and preventing it from reaching the bed. The absence of esker ridges at the final location of ice divides is rather abrupt (Fig. 6), and the total width of the esker-free area is relatively constant at 100—150 km. This distance may relate to an underlying control on how far from ice divides eskers can form, perhaps related to the hydraulic potential and meltwater supply, or the availability of a sufficient quantity of sediment to build eskers.

Theoretical work has shown that the ice surface topography (and, to a lesser extent, the basal topography) dictates the potential gradient followed by englacial and subglacial meltwater channels (Shreve, 1972). Moreover, Shreve (1985a; b) and Syverson et al. (1994) demonstrated that esker paths are likely to be dictated, at least in part, by the potential gradient. Whilst it is beyond the scope of the present paper to match esker paths to reconstructed potential gradients, it is likely that the ice surface exerted an influence on esker locations, most likely in association with the other controls

discussed above. We emphasise this as an important area for future work (see Section 5.7).

No instances of cross-cutting eskers were found in the mapping, which contrasts markedly with the abundance of cross-cutting lineations found on the LIS bed (e.g. Boulton and Clark, 1990; Stokes et al., 2009; Brown et al., 2011). This suggests that eskers have a low potential for preservation beneath dynamic ice sheets, and/or that they form very close to final deglaciation. Elsewhere, eskers have been shown to survive entire glaciations beneath frozen beds (Lagerbäck and Robertsson, 1988; Kleman, 1994) and frozen beds have been inferred beneath parts of the LIS (Kleman and Hättestrand, 1999; Kleman and Glasser, 2007), although the subglacial thermal regime changes through time to almost entirely warm-based (e.g. Marshall and Clark, 2002). As a result of these significant changes in thermal regime, as well as significant changes in ice dynamics (e.g. Boulton and Clark, 1990), it is unlikely that eskers in Canada would survive an entire glacial cycle. Moreover, eskers require a significant input of meltwater in order to form, meaning that this is more likely to occur during deglaciation, when surface melting is a significant process (Mooers, 1989; Carlson et al., 2009) and the probability of preservation at this time is also largest, since there is no subsequent ice flow to erode them. For these reasons, eskers are frequently interpreted as deglacial landforms and are often used to reconstruct deglaciation (e.g. Dyke and Prest, 1987; Dyke et al., 2003; Stokes et al., 2009; Margold et al., 2011, 2013; Clark et al., 2012).

In summary, the pattern of eskers on the bed of the LIS points to a dichotomy between complex ice dynamics in the outer reaches of
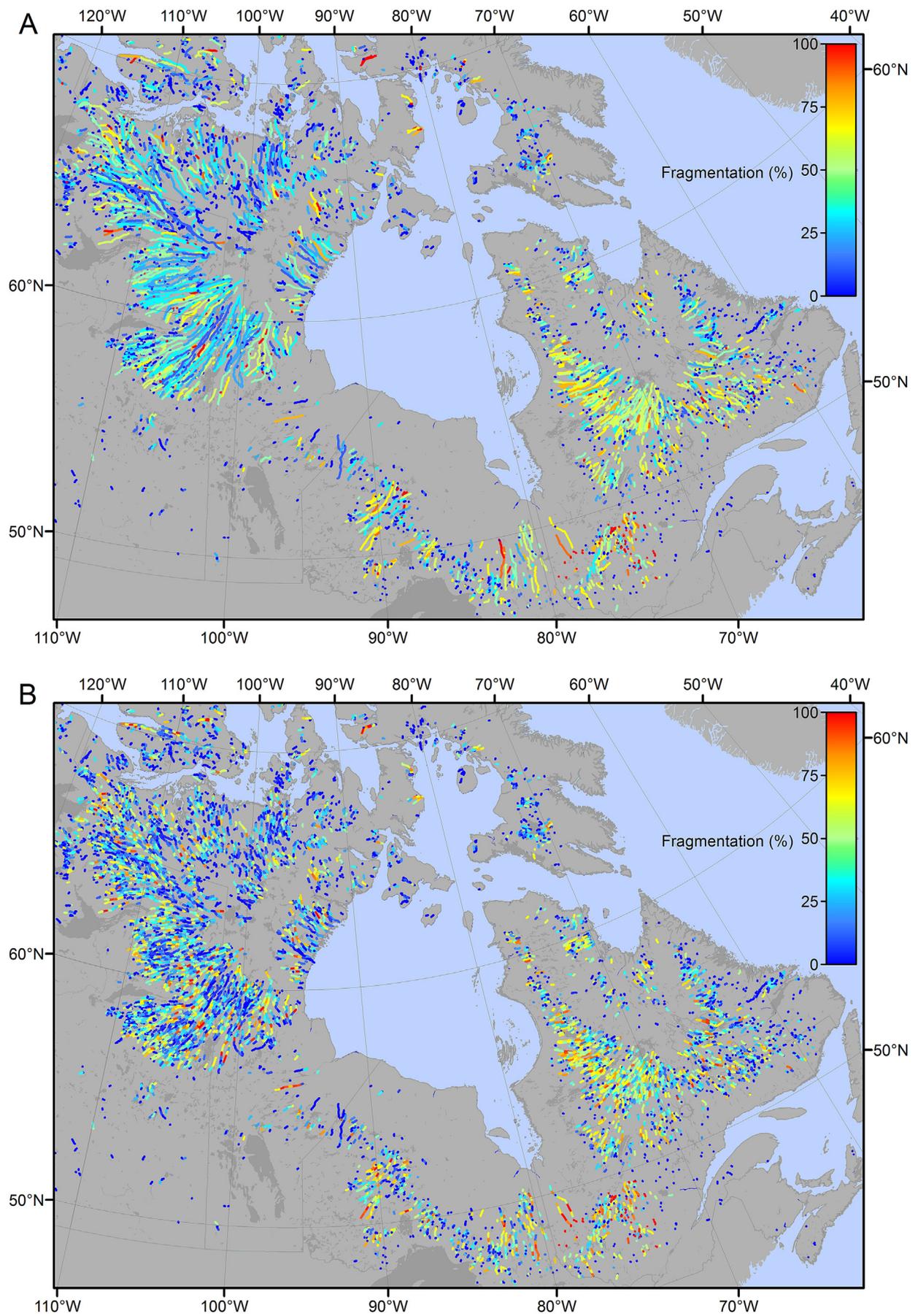
Fig. 12. A) Map of *interpolated* eskers classified by fragmentation (the percentage of the esker that was interpolated) for each esker. B) Map of *interpolated* eskers classified by fragmentation for each 20 km segment of eskers (N.B. 100% fragmentation is possible if an interpolation was made over 20 km). Note the higher fragmentation of the eskers of Quebec (east), in comparison with the eskers of Keewatin (west).
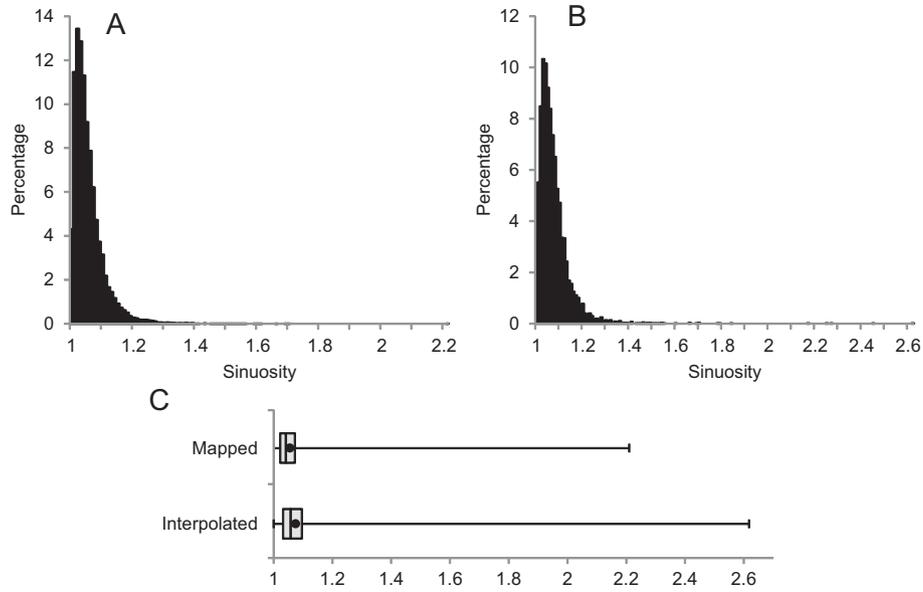
Fig. 13. Histograms of esker sinuosity for (A) *mapped* esker ridges ($n = 20{,}186$, 0.01 bins) and (B) *interpolated* eskers ($n = 5{,}932$, 0.01 bins). C) Box and whisker plot comparing the two distributions. Whiskers denote the range of values, points denote means and the boxes span the range of the 25—75% percentiles, with the median as a vertical bar.
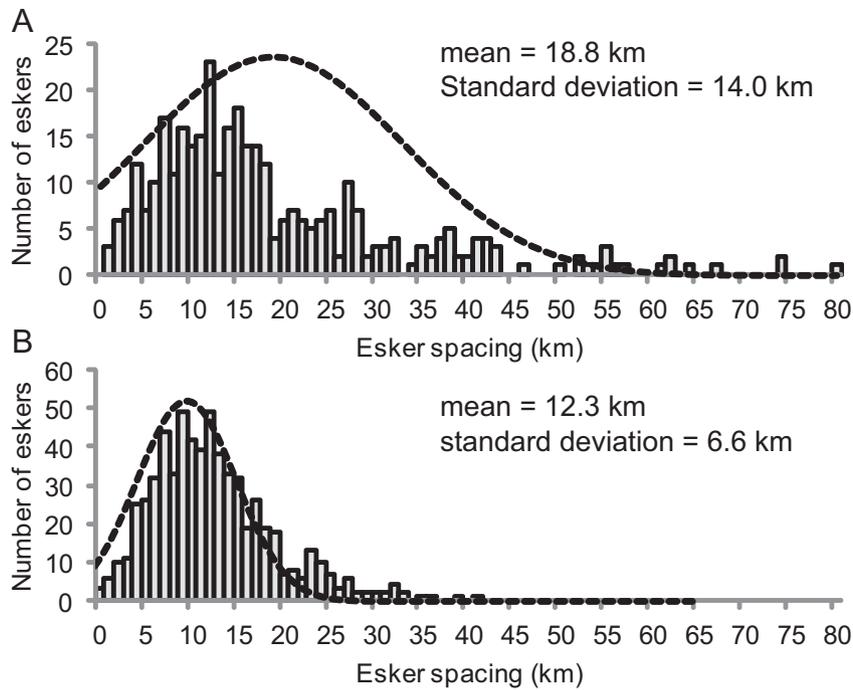

Fig. 14. Histograms of esker spacing (1 km bins) for the three test areas (see Fig. 6). Dashed lines are normal distributions with the same mean and standard deviation as the data. A) *Mapped* eskers ($n = 347$). B) *Interpolated* eskers ($n = 632$).

Table 1
Spacing statistics for each study area (see Fig. 6). Note the lower standard deviation values associated with *interpolated* eskers.

| Location	No. of spacing measurements		Mean spacing		Standard deviation	
	Mapped	*Interpolated*	*Mapped*	*Interpolated*	*Mapped*	*Interpolated*
1. Northwest Territories (40,000 km²)	138	224	17.0 km	12.1 km	12.6 km	6.4 km
2. Northern Saskatchewan (40,000 km²)	113	209	19.5 km	12.4 km	14.9 km	6.9 km
3. Quebec (40,000 km²)	96	200	20.7 km	12.4 km	14.7 km	6.6 km
1,2 and 3 combined (120,000 km²)	347	632	18.8 km	12.3 km	14.0 km	6.6 km
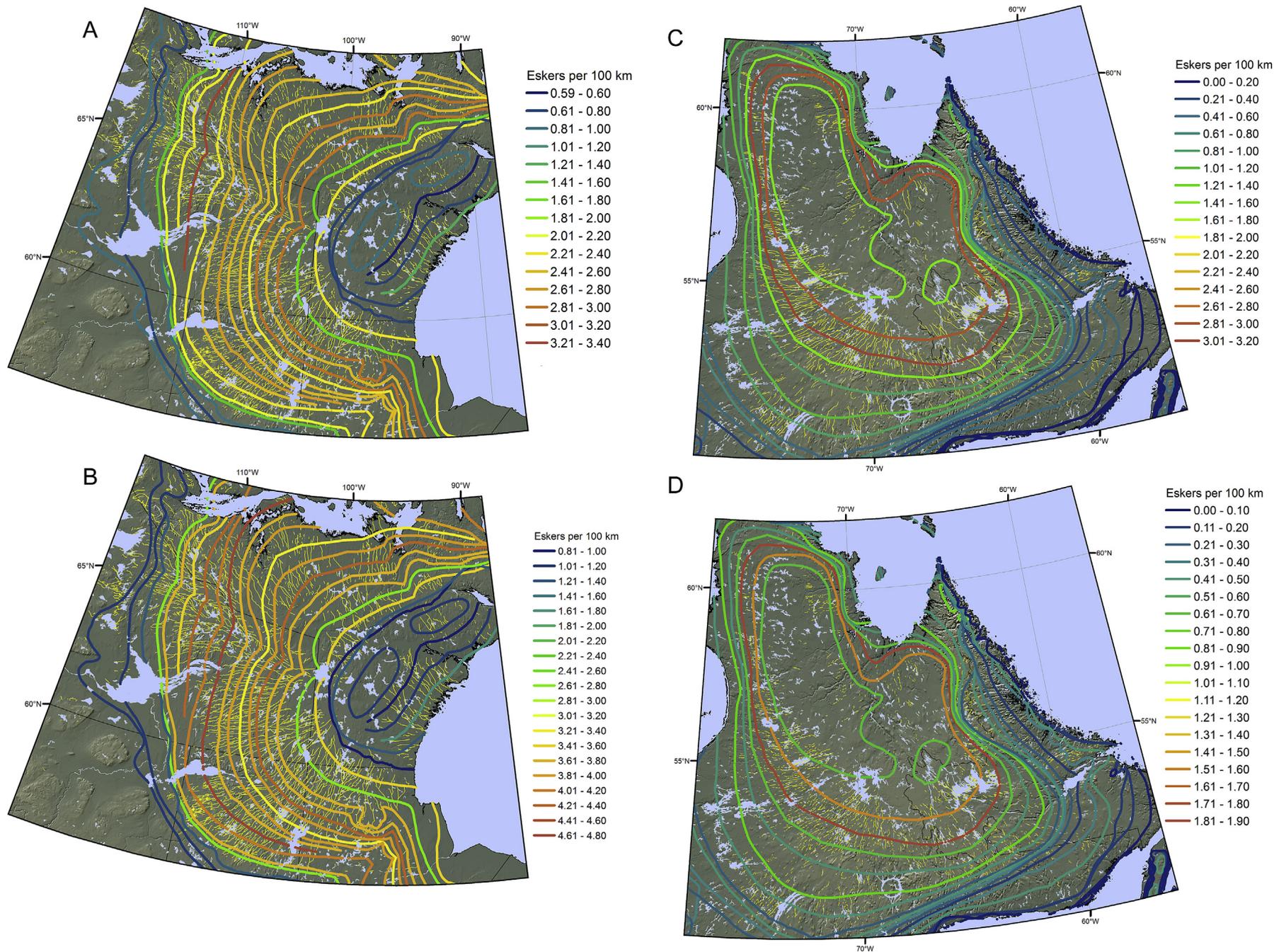
Fig. 15. Esker density around the Keewatin (A and B) and Labrador (C and D) sectors, derived from (A and C) *mapped* eskers; and (B and D) *interpolated eskers*. Ice margins are coloured based on esker density. (For interpretation of the references to colour in this figure legend, the reader is referred to the web version of this article.)
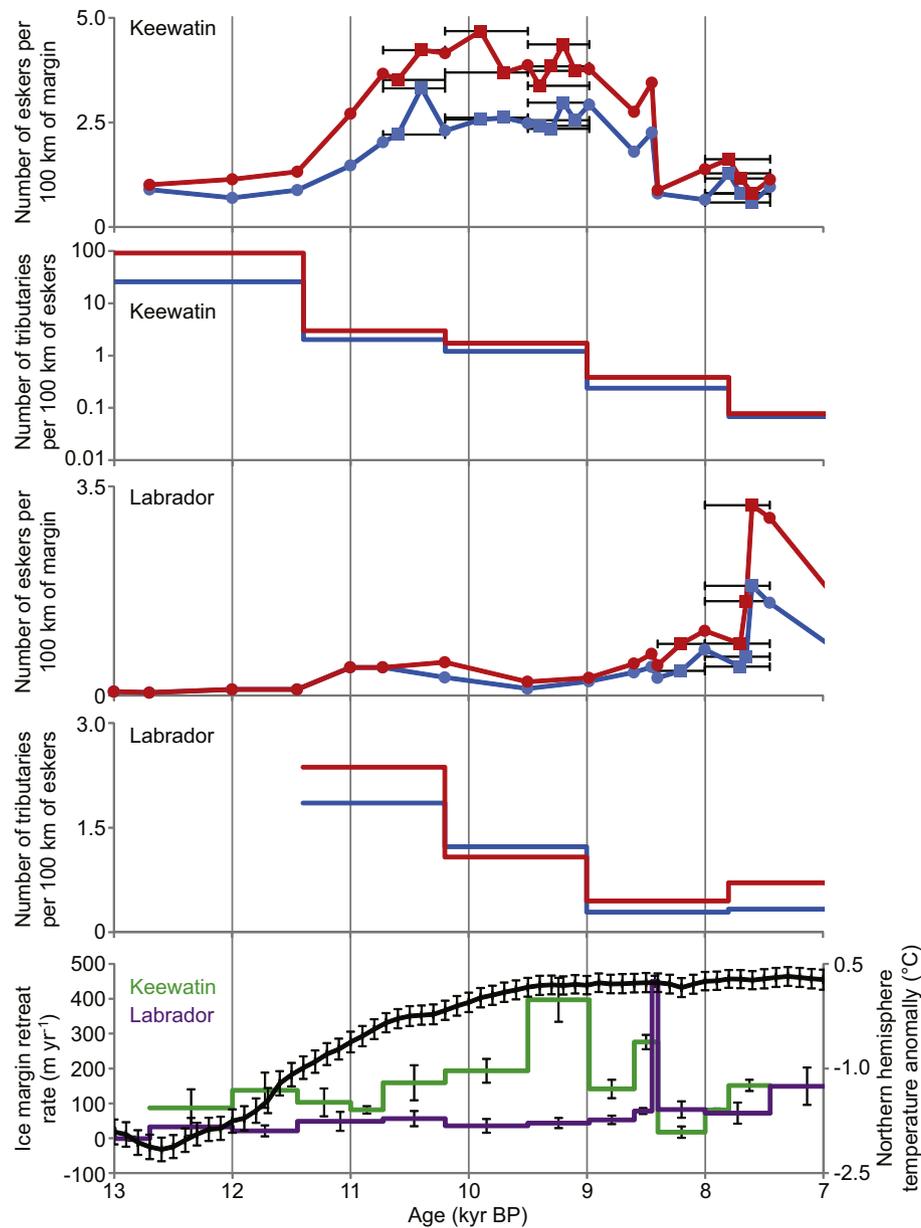
Fig. 16. Changes in esker density and tributaries through time. Error bars on the intermediate margin points (squares rather than circles) denote the two margins between which the new margin was interpolated. Red denotes *interpolated* eskers and blue denotes *mapped* eskers. Note that the tributary data for the Keewatin sector are plotted on a $\log_{10}$ *y*-axis to accommodate the large values between 11.5 and 13 ka BP. The northern hemisphere temperature record is from Shakun et al. (2012) and shows the temperature anomaly from the early Holocene (11.5–6.5 ka BP) mean. Error bars indicate 1σ uncertainty. The mean retreat rate of the ice sheet in each sector is given with 1σ error bars ($n = 20$). *Mapped* esker data after Storrar et al. (2014). (For interpretation of the references to colour in this figure legend, the reader is referred to the web version of this article.)

the LIS during early deglaciation, which led to the formation of visually 'chaotically' arranged eskers in the outer reaches of the ice sheet, and the relatively simple retreat of the ice sheet over the harder bed of the Keewatin and Labrador sectors, which led to the

formation of more 'organised' eskers. The concentration of eskers on the Canadian Shield is likely a product of the hydrogeological properties of the rocks (which were more conducive to R-channel formation) and the spatial coincidence of the Shield with the final location of the ice sheet during the later stages of deglaciation, when the supply of meltwater was very large. This provides a useful framework for interpreting patterns of eskers on other ice sheets beds.

5.2. Esker length

Mean esker ridge length (3.5 km) is comparable to data from the UK and the Kola Peninsula (Table 3), although the maximum length of Canadian esker ridges is much larger, which likely reflects the larger size of the LIS and the stability of meltwater conduits in both

Table 2
Total length of first-to fourth-order eskers.

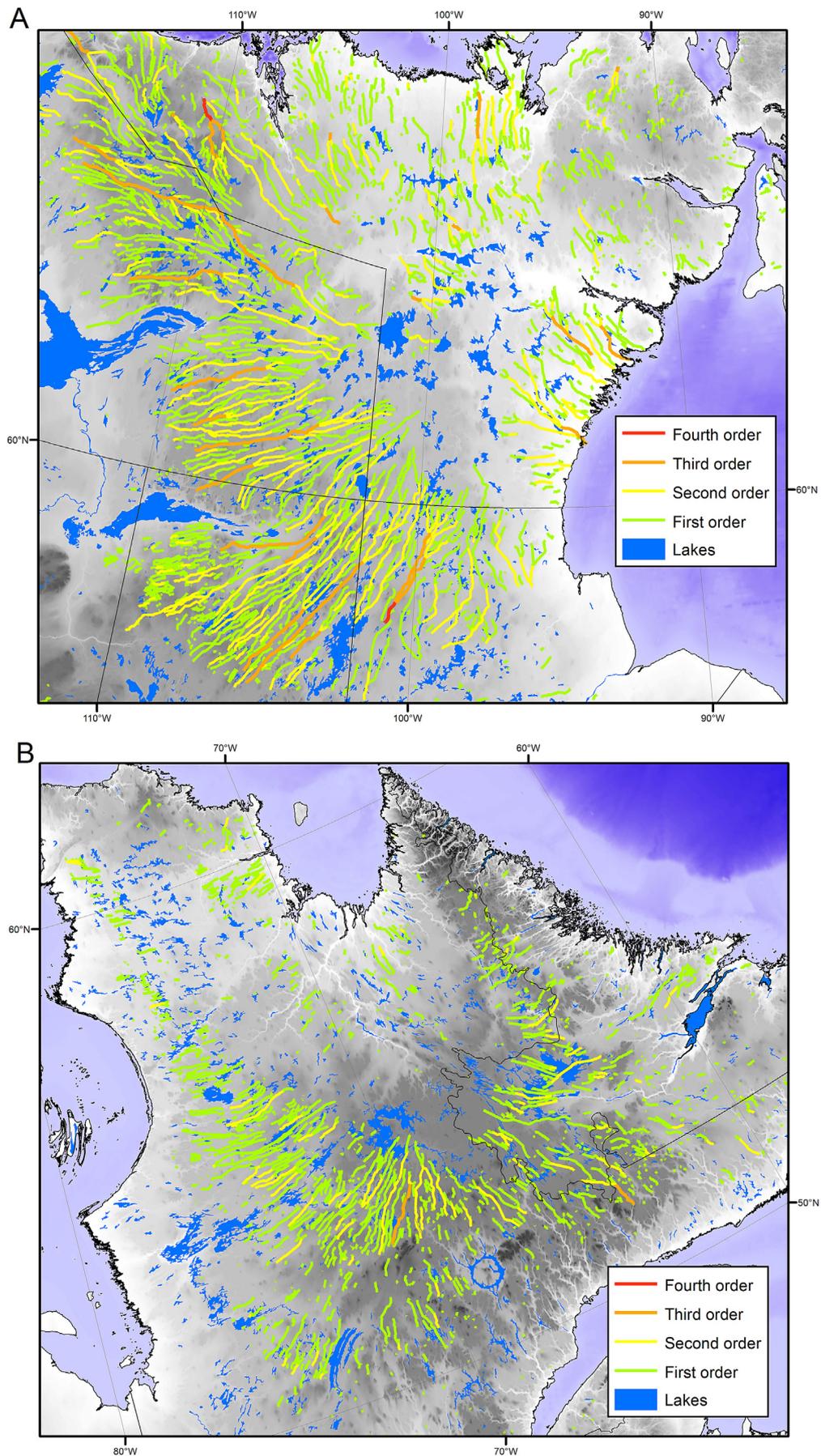| Strahler number	Total length (km)	Percentage of total	Total length (km)	Percentage of total
	mapped	*mapped*	*interpolated*	*interpolated*
1	68,785	96.472	824,268	74.999
2	2512	3.524	232,848	21.187
3	3	0.004	41,823	3.805
4	0	0	98	0.009

Fig. 17. Strahler numbers calculated for *interpolated* eskers in (A) the Keewatin sector and (B) the Labrador sector. Note that fourth-order eskers are developed in two locations in Keewatin.
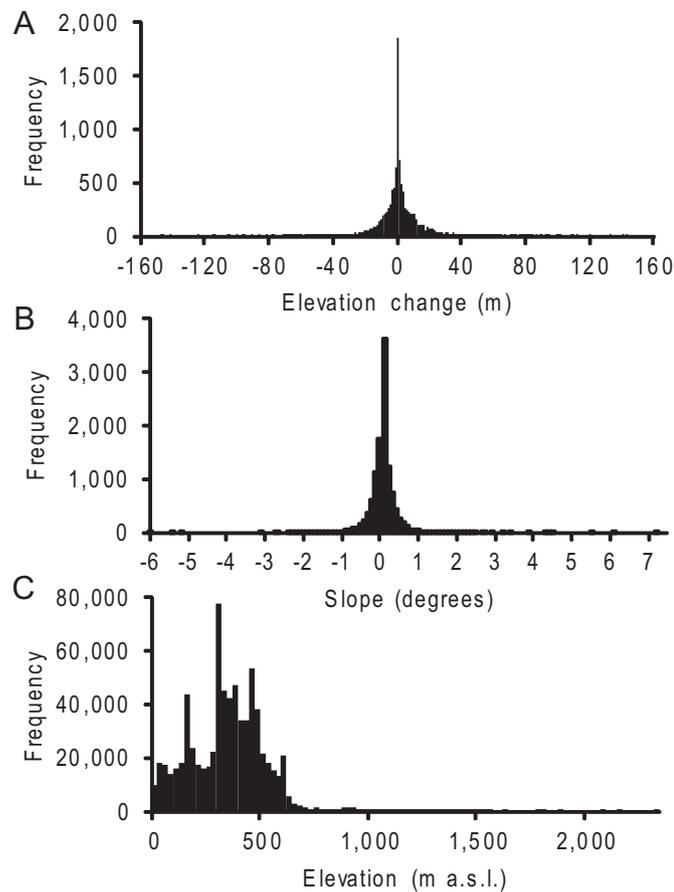
Fig. 18. A) Histogram of elevation change values (1 m bins) for esker ridges in the Keewatin and Labrador study areas (see Fig. 6 for locations; n = 11,562). Positive values denote esker ridges trending uphill and negative values indicate a downhill trend. B) Histogram of slope values (0.1° bins) for esker ridges in both areas. Positive values denote esker ridges trending uphill and negative values indicate a downhill trend. C) Histogram of elevation values for points every 100 m along each esker ridge for all of Canada (n = 20,186 esker ridges; 722,834 point measurements).

space and time. Esker length, like that of other glacial landforms (Clark et al., 2009; Hillier et al., 2013; Stokes et al., 2013), follows a log-normal distribution. Unlike other landforms, however, this likely reflects the fact that long eskers (e.g. >100 km) are frequently broken into many shorter esker ridges, rather than different eskers 'growing' to different lengths, as has been suggested for drumlins (e.g. Clark et al., 2009; Spagnolo et al., 2012).

Eskers are typically less than 10 km long and are broken by small gaps. The reason for this fragmentation is either a cessation in sedimentation, or post-depositional erosion (Banerjee and McDonald, 1975). Erosion may arise from dissection by subsequent meltwater flow or contemporary rivers, or inundation by lakes formed either during deglaciation, or by later thermokarst processes (e.g. Smith et al., 2005; Smith et al., 2007; Jones et al., 2011). Fig. 11 reveals that eskers associated with the Labrador sector of the LIS are significantly more fragmented than those of the Keewatin sector. A potential explanation for this is that the ice dynamics during the final stages of deglaciation were markedly different in these two sectors of the ice sheet. Whilst the Keewatin sector generally experienced the gradual retreat of a terrestrially-terminating margin (Aylsworth and Shilts, 1989a; Dyke et al., 2003), ice in the Labrador sector switched from being marine-to terrestrially-terminating, encompassing destabilisation and rapid retreat as it did so (Hillaire-Marcel and Occhietti, 1980; Clark et al.,

2000). If eskers form time-transgressively, they are more likely to be continuous (i.e. less fragmented) if the margin retreats slowly, as in Keewatin. Conversely, if the margin retreats rapidly, as it did in Labrador, there is less time for eskers to be deposited and so they become more fragmented, with larger segments forming when the margin is more stable.

Once these gaps are accounted for, eskers may be traced for up to 760 km. This indicates that deposition took place rapidly in very long conduits (e.g. Brennand and Shaw, 1994, 1996) which potentially reflects the extent of the ablation zone and surface melting (e.g. Weertman, 1972), or that conduits were stable through time and were filled time-transgressively by depositional processes (e.g. Banerjee and McDonald, 1975; Gorrell and Shaw, 1991; Boulton et al., 2009). In either case, the processes responsible for 'long' ($\gtrsim$100 km) esker formation require explanation, because they imply a large-scale control on meltwater conduits which has not been described elsewhere.

Observational and sedimentological evidence has demonstrated that shorter (up to a few 10s of km) eskers can form synchronously (Brennand, 1994; Brennand and Shaw, 1996; Brennand, 2000; Burke et al., 2008, 2009, 2010). It is unlikely, however, that the longest eskers formed synchronously in (up to) 760 km long conduits. Synchronous deposition would require a very large quantity of meltwater and sediment to abruptly enter the drainage system during early deglaciation (around or prior to 12 ka BP), and then be preserved throughout deglaciation, with no further meltwater drainage being recorded in the geomorphological record. Rather, we favour the parsimonious explanation that very long eskers were built time-transgressively at a retreating ice margin. This explanation allows for the gradual formation of eskers as and when sediment and meltwater become available throughout deglaciation, and does not require large 'pulses' of sediment and meltwater in a single, very long conduit. Moreover, time-transgressive deposition means that eskers were formed at the margins of the ice sheet and would not then have to survive overriding during deglaciation.

A key question regarding time-transgressive formation of long eskers is: what process is responsible for the deposition of continuous, long eskers over such a long distance (several hundred km) and time (several thousand years)? In other words, how can conduits persist at a particular relative position in an ice margin throughout the deglaciation of the ice sheet? Long eskers predominate in areas where deglaciation was relatively uniform (i.e. on the Canadian Shield in the Keewatin sector: Fig. 11), which helps to explain how the conduit positions changed relatively little during deglaciation, because the geometry and ice flow trajectories of this sector of the ice sheet did not change significantly, apart from becoming smaller (Dyke et al., 2003). However, the locations of conduits relative to the ice margin would be expected to evolve as the hydraulic gradient, imposed (in part) by the pressure of overlying ice, changed as the ice sheet shrank (cf. Shreve, 1972). The presence of several long eskers around the Keewatin sector points to a balance between these processes, i.e. long eskers were deposited in conduits maintained by the geometry of the ice sheet, their paths reflecting the migration of the hydraulic gradient as the pressure regime in the ice sheet evolved during deglaciation. Surrounding shorter eskers may reflect locations where conduits were no longer maintained as they became 'out-competed' by larger conduits. An important consideration is the nature of the conduits themselves. R-channels operate at relatively low pressure and capture meltwater from their surroundings (Röthlisberger, 1972). The largest R-channels would therefore be likely to maintain a relatively stable position relative to the ice margin, as the largest channels would capture meltwater from surrounding smaller ones. This is similar to the self-organising processes proposed by Boulton et al. (2009) and Hewitt (2011) to dictate the spacing between
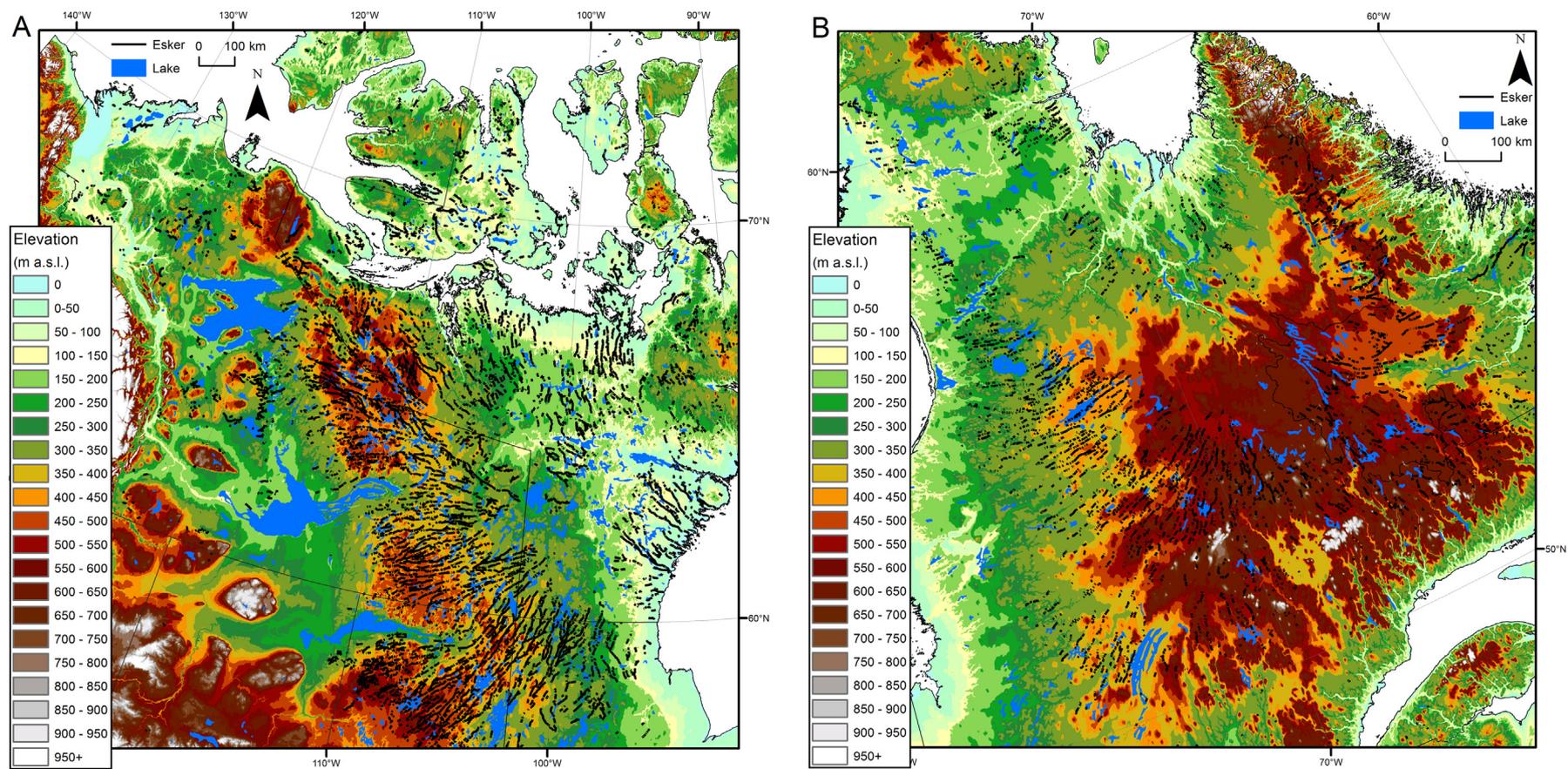
Fig. 19. *Mapped* eskers displayed against topography, shaded in 50 m intervals, for (A) the Keewatin area and (B) the Labrador area. (For interpretation of the references to colour in this figure legend, the reader is referred to the web version of this article.)

Table 3
Comparison of length and sinuosity statistics. UK data are from Clark et al. (2004) and Kola Peninsula data are from Hättestrand and Clark (2006).

	UK (n = 857)	Kola Peninsula (n = 817)	Canada (n = 20,718
Mean length (km)	1.0	3.1	3.5
Maximum length (km)	18.2	9.9	97.5
Mean sinuosity	1.03	1.06	1.06
Maximum sinuosity	1.36	1.38	2.21

channels. This type of mechanism explains why there are eskers several hundred km long (the larger R-channels), alongside systems of smaller eskers, which likely occupied the gaps between drainage divides of the largest R-channels and did not scavenge as much meltwater.

5.3. Esker sinuosity

Esker ridge sinuosity is very small. Mean sinuosity is 1.06 and few values attain more than 1.20. Mean sinuosity is in accordance with data from other areas (e.g. Clark et al., 2004; Hättestrand and Clark, 2006; Burke et al., 2012), but maximum sinuosity is higher, likely due to the large sample size (Table 3). Sinuosity is significant because it is an important parameter for dye-tracing experiments and numerical models of subglacial channels. Variations in sinuosity can profoundly influence the outcome of such experiments because sinuosity has implications for the length of a channel between two points and, consequently, the discharge, volume, pressure and velocity of the contained water. For example, one attempt to incorporate estimates of sinuosity into a model of tracer velocity through a subglacial channel (Schuler and Fischer, 2009), suggests a sinuosity value of 1.6 as being the most realistic for an R-channel under Unteraargletscher, Switzerland. Whilst this applies to an alpine glacier, our data suggest that R-channels are significantly straighter under ice sheets. Thus, we suggest that models of subglacial channels at the ice sheet scale should assume sinuosity values on the order of 1.06 to achieve the most realistic results.

Understanding why eskers are so straight is also important for understanding the processes controlling subglacial channel characteristics. When sinuosity is plotted against length, it becomes apparent that the longest eskers are consistently among the straightest and, conversely, that the shortest eskers are the most sinuous (Fig. 20). This is the opposite of the effect mentioned in Section 3.2.2, whereby sinuosity decreases for small fragments of

larger eskers. The effect discussed in Section 3.2.2 is related to the fragmentation of eskers, whereas the observation of long, straight eskers in Fig. 20 suggests that there is a different process which modulates the straightness of very long channels and allows shorter channels to be more sinuous.

Short eskers (e.g. <10 km) likely reflect deposition close to the ice margin (assuming they were formed time-transgressively) and, as such, were probably formed in conduits under atmospheric pressure, rather than hydrostatic pressure (which would be expected further up-ice: Röthlisberger, 1972; Shreve, 1972). Slope data does not contradict this, in that approximately 50% of eskers trend downhill and could, therefore have been at atmospheric pressure. Conduits under hydrostatic pressure would be more likely to erode a straight channel through the ice because of the increased friction associated with the pressurised water (cf. Röthlisberger, 1972). Thus, long conduits under hydrostatic pressure would likely lead to the development of straighter eskers. Conversely, if the shorter eskers forming closer to the ice margin were deposited under atmospheric pressure, they would be expected to produce a more meandering planform because their course would be dictated more by local factors such as obstacles or basal topography. Many shorter eskers, however, are still very straight, which is potentially related to the tendency of channels to follow structural weaknesses in ice, which would promote the formation of straight channels (cf. Gulley and Benn, 2007; Gulley, 2009; Gulley et al., 2009a, b). This further supports our interpretation that the longest eskers represent the most stable (time-transgressive) conduits, as dictated by the geometry and hydraulic gradient of the ice sheet (see Section 5.2). Note, however, that the lack of variation in sinuosity values for esker ridges means that sinuosity values cannot be used to discern variations in discharge or sediment load of the channels in which they formed, in contrast to some fluvial systems (Schumm, 1963; Makaske, 2001).

5.4. Lateral spacing

Measurements of *interpolated* esker spacing in three sample areas where esker density is high, indicate that eskers are very regularly spaced, as also suggested by previous work (see Fig. 4). Regular esker spacing has also been observed at modern glaciers (Boulton et al., 2007a). Mean spacing of Canadian (*interpolated*) eskers is 12.3 km with a standard deviation of 6.6 km, in agreement with figures from the literature (Fig. 4). The three areas selected are ideal for testing numerical models because the *interpolated* esker dataset has few gaps, laterally or longitudinally and so we assume
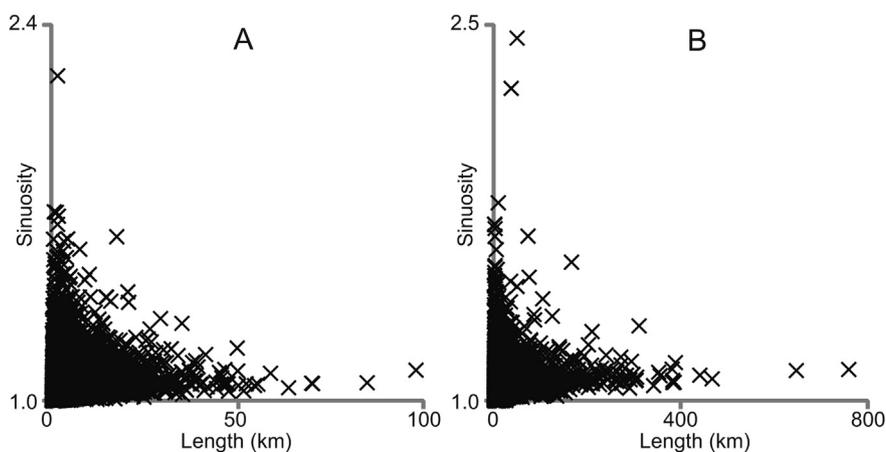

Fig. 20. Esker length plotted against sinuosity for (A) *mapped* (n = 20,186) and (B) *interpolated* (n = 5932) eskers.

that they reflect the locations of all R-channels in the area. Thus, models can be directly compared with observations and, in this regard, preliminary results are encouraging. Boulton et al.'s (2007a, b, 2009) model produced spacing values of 8–25 km in Scandinavia and Hewitt's (2011) model produced an estimated spacing of 5–30 km. According to Boulton et al.'s (2007a, b, 2009) model, esker spacing is primarily controlled by the transmissivity of the substrate and the basal melt rate of the ice sheet. Permeability on the Canadian Shield is estimated to be on the order of 8.9×10^{-16}–3.2×10^{-13} m^2 (Gleeson et al., 2011), which is comparable to transmissivity of 1.8–6.4×10^4 m^2 yr^{-1} for a substrate 10 m in thickness. Boulton et al. (2009) suggest that transmissivities of 10^{-1}–10^4 m^2 yr^{-1} in Scandinavia are sufficient to be significant in draining meltwater beneath ice sheets. Thus, it appears to be feasible that the groundwater theory may be applicable to the eskers of Canada.

Supraglacial melting presents an important supply of meltwater in addition to basal melting, particularly during deglaciation (Carlson et al., 2009), and is considered here in addition to basal melting as an important factor in determining esker spacing. Increasing the transmissivity or decreasing the basal/supraglacial melt rate results in more widely spaced eskers. Thus, given our observation of eskers closer together further toward the centres of deglaciation, this implies that melt rates were likely higher as the LIS deglaciated, which corroborates the results of a surface energy-mass balance model (Carlson et al., 2009). In Hewitt's (2011) model, eskers become more widely spaced when the potential gradient is smaller or the permeability of the distributed system is larger. This also suggests that more water entered the drainage system during deglaciation of the LIS. The promising agreement between model predictions and esker spacing data may be tested further, by assessing variations in esker spacing over different hydrogeological units to assess whether the hypothesis of Boulton et al. (2009) is applicable at large scales and to better understand whether esker spacing is controlled by basal or supraglacial meltwater sources, or a combination of both.

5.5. Density and tributaries during deglaciation

An analysis of the changes in esker density through time reveals that, in central-western Canada, esker density increased rapidly between 12 and 9 ka BP, coinciding with the rapid retreat of the ice sheet between the end of the Younger Dryas (~11.5 ka BP) and 8.5 ka BP (Dyke et al., 2003; Carlson et al., 2008). Storrar et al. (2014) argued that this reflects the increased meltwater supply from surface melting as the LIS retreated. As more meltwater became available, more esker-forming channels were produced, which may indicate that a greater percentage of the LIS bed was drained by channels. Theoretical work suggests that as the meltwater discharge increases, R-channels increase in size, since the frictional melting imparted by the high discharge outweighs closure of the channels by ice creep (Röthlisberger, 1972). Thus, measurements of esker width (not presented here) may provide further insights into the supply of meltwater during deglaciation. More recently, Boulton et al. (2009) suggested that increased meltwater discharge may result in more closely spaced R-channels, a prediction which does match our observations here.

The increase in esker density during deglaciation is also likely to be linked to the changing surface profile of the ice sheet as it retreated. In the final stages of deglaciation, a large portion of the ice sheet is likely to have been beneath the equilibrium line (Carlson et al., 2009) and the low-profile ice sheet would therefore have experienced significant melting, and the increased potential to create eskers.

Up-glacier of the 8.5 ka BP margin, esker density decreased, coinciding with the point at which the retreat rate of the ice sheet/

cap decelerated or stabilised (Carlson et al., 2008). Few eskers were formed in the final stages of deglaciation, which might be explained by the existence of cold-based ice beneath the residual ice caps during final deglaciation (Kleman and Hättestrand, 1999; Kleman and Glasser, 2007; Storrar et al., 2014), or an insufficient supply of meltwater and/or sediment to form the eskers, again related to the smaller size of the ice mass.

In eastern Canada, the pattern is slightly different, presumably a product of the separation of the Keewatin and Labrador domes into two ice caps at about 8.5–9 ka BP and the different ice sheet-climate dynamics in each sector (Hillaire-Marcel and Occhietti, 1980; Clark et al., 2000; Dyke et al., 2003; Carlson et al., 2008). Esker density in Labrador was relatively stable (between 0 and 0.76 eskers per 100 km of ice margin) until ~7.6 ka BP, when it increased markedly until final deglaciation. This matches the changes in ice sheet retreat rate (although the volume of ice will decrease at a different rate), which are in agreement with observations that this sector of the ice sheet was relatively stable until approximately 9 ka BP (Dyke et al., 2003), when it began to retreat more rapidly, explaining the lag in the increased esker density compared with the Keewatin sector. The stability of the ice margin until ~9 ka BP and relatively small number of eskers in the outer sections of this sector of the ice sheet explain the very high values of esker spacing up to 11 ka BP (Fig. 16). Thereafter, a similar pattern to the Keewatin sector is observed, esker density increasing to accommodate the additional channels as the supply of meltwater increased.

Whilst esker density increased during deglaciation, the relative proportion of tributaries decreased. If the increased density of eskers during deglaciation was the result of increased upstream branching in dendritic systems, one would expect the proportion of tributaries to increase through time. This is not the case and provides support for the interpretation that increased esker density is related to increased channelisation of the meltwater drainage system (Storrar et al., 2014). Alternatively, if laterally divergent flow was dominant during the later stages of deglaciation, this would impose a strong topographic control on flow direction, potentially unfavourable for the development of tributaries. It should be noted that we only provide direct evidence here for the increase in *channelised* drainage, and that no inference can be made about the nature of the hydrological system that did not result in the formation of eskers, for example if it was drained by canals (e.g. Walder and Fowler, 1994) or a system of linked cavities (e.g. Lliboutry, 1969).

5.6. Topography/slope

Until now, there have been few reports of elevation changes in eskers (see section 2.6). Theory suggests that eskers form in accordance with the hydraulic gradient, which is related to ice surface topography and bed topography (Shreve, 1972, 1985a, b). If water pressure equals ice overburden pressure (i.e. flotation), the slope of the ice surface exerts 11 times the influence of the bed slope in controlling the direction of water movement (Shreve, 1985a). This value is less, however, if water pressure (P_w) is lower than ice overburden pressure (P_i), which is expressed by the 'flotation ratio' (f_w):

$$f_w = P_w / P_i \tag{4}$$

When $f_w = 0.56$, surface and bed slopes exert an equal influence on water direction (Cuffey and Paterson, 2010). Thus, for values of f_w less than 0.56, water is less likely to ascend topographic slopes, and *vice versa*. Esker elevation data reveal that an equal proportion of Laurentide eskers trend up- and down-slope, therefore suggesting that at least half of the conduits in which these eskers formed were close to ice overburden pressure.
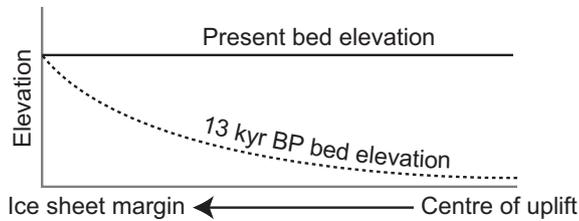
Fig. 21. Schematic illustration of the effect of glacio-isostatic adjustment on esker elevation. Areas of presently flat topography represent areas of adverse slope of the ice sheet bed when eskers were formed, suggesting that eskers which lie on presently flat terrain may have formed on primarily up-hill slopes, depending on the amount of uplift since esker formation.

It is important to note that the elevation values presented here are not corrected for glacio-isostatic adjustment (GIA), which may skew the results where long eskers stretch from areas of pronounced uplift (especially in the Keewatin sector) to areas of more subdued uplift (see Peltier, 2004; Dyke et al., 2005). The effect of GIA also has implications for the nature of the bed on which the eskers formed, compared with the bed observed today. For example, areas of flat terrain at present likely represent former adverse slopes, because more uplift will have occurred towards the central parts of the ice sheet than towards the periphery (Fig. 21). Total uplift since 13 ka BP (the isochrone corresponding to the outer reaches of the Keewatin and Labrador eskers) is shown in Fig. 22 (Peltier, 2004) and slope profiles along eight transects, where the longest esker systems are located, are plotted for the basal topography at 13 and 0 ka BP in Fig. 23, revealing that GIA has had a minimal impact on the gradient of the bed in most cases.

5.7. Future work

This paper presents a preliminary analysis of our database of esker morphometry and pattern. In addition to the results presented here, the data are particularly well suited to several areas of potential future research. For example, the locations of eskers could be statistically compared with meltwater drainage pathways

predicted by ice sheet models (e.g. Livingstone et al., 2013), similar to (but on a much larger scale than) the work of Shreve (1985a). The database could also be used alongside geological data to assess lithological and hydrogeological controls on esker location, which have been hypothesised by several workers (e.g. Aylsworth and Shilts, 1989a; Clark and Walder, 1994; Grasby and Chen, 2005; Boulton et al., 2009). The data may also be used, alongside other landforms, to refine our understanding of the configuration of the ice margins of the Laurentide Ice Sheet as it deglaciated, as has recently been done in the UK (Clark et al., 2012). Finally, the slope data for each esker ridge may be compared with the local isostatic rebound curve to further investigate the former bed topography when the eskers were formed and also to provide further insights into the subtleties of GIA that coarser-resolution models are unable to evaluate.

6. Conclusions

The subglacial meltwater drainage systems of ice sheets are an important but difficult environment to observe. This paper presents the first quantitative analysis of the morphometry of a large sample (over 20,000) of eskers in Canada, which is used to provide key insights into the properties of the subglacial drainage systems of the LIS. Canadian eskers exhibit several patterns at different scales. They radiate outwards in the location of the two main ice domes, and are absent beneath the final ice divides in areas of 93,000 and 174,000 km^2 in Keewatin and Labrador, respectively. The esker free areas are 100–150 km wide in both locations. Within the radial esker systems, they form integrated dendritic networks of up to fourth order tributaries. Elsewhere, and off the Canadian Shield, eskers are more chaotic, likely reflecting a lack of stable R-channel formation and complex ice dynamics related to ice streaming over soft sediments.

The longest contiguous esker ridge is 97.5 km and most eskers are between 0 and 10 km long. Gaps between eskers are numerous (mostly due to lake infilling), but when they are conservatively interpolated over distances of just a few kilometres, esker systems extend up to 760 km. This suggests that eskers either formed synchronously in channels up to 760 km long, or time-
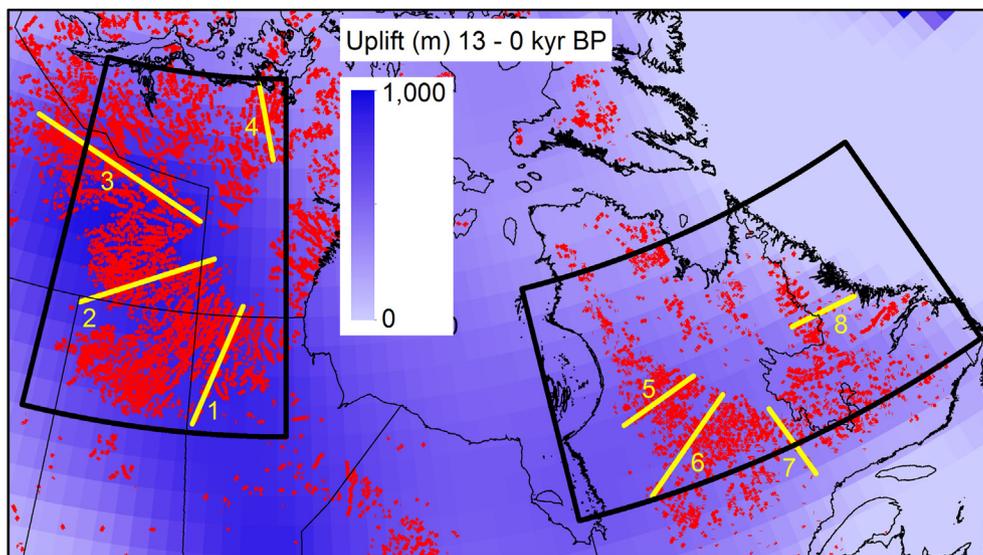

Fig. 22. Total isostatic uplift from 13 ka BP to present from the ICE-5G (VM2 L90) model (Peltier, 2004). Eskers are shown in red and the Keewatin and Labrador areas used to determine esker elevation changes (as in Fig. 18) are shown by black boxes. Negative values (offshore and not associated with eskers) are not shown. The yellow numbered lines indicate the locations of the transects used to produce the plots in Fig. 23. (For interpretation of the references to colour in this figure legend, the reader is referred to the web version of this article.)
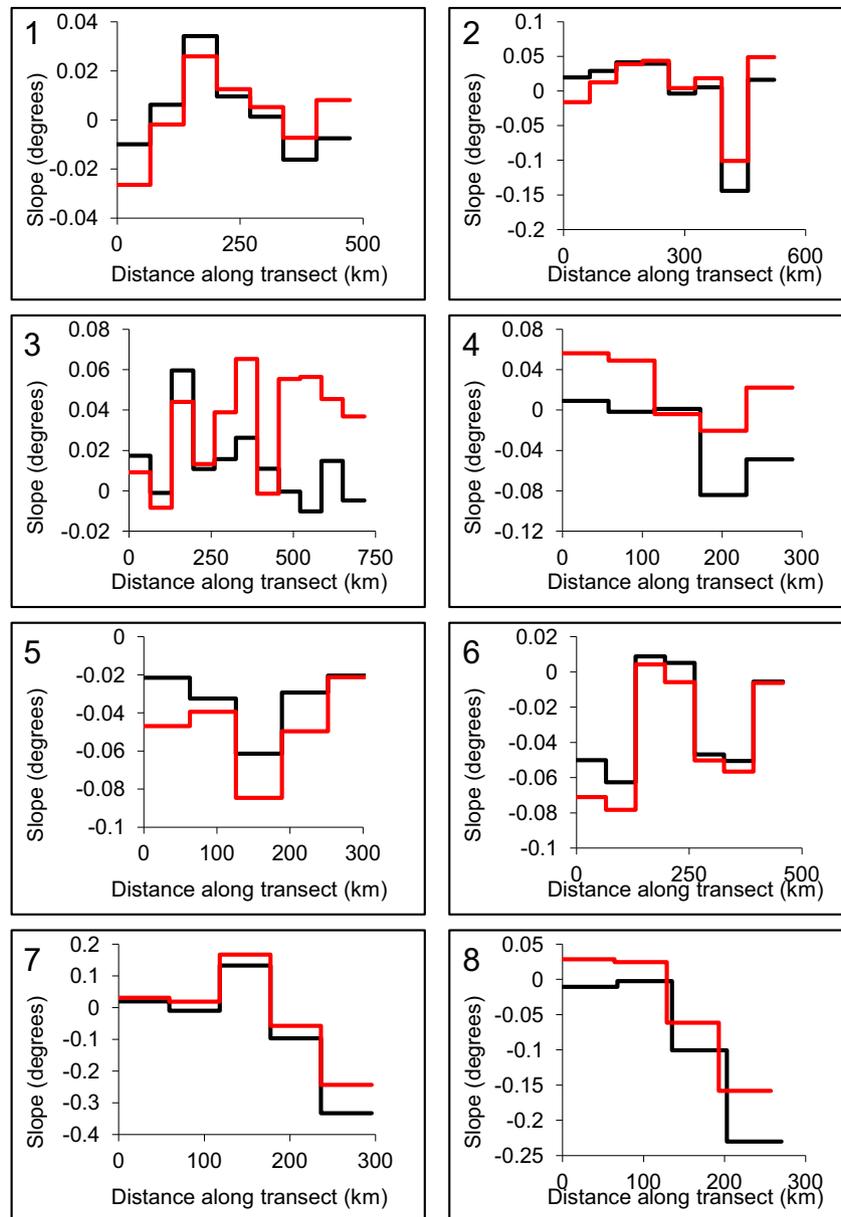
Fig. 23. Slope profiles along the transects shown in Fig. 22 for the ice sheet bed at 0 ka BP (black lines) and 13 ka BP (red lines). The distance along the transect increases towards the margins of the ice sheet. Negative slopes indicate a fall in elevation towards the periphery of the ice sheet. (For interpretation of the references to colour in this figure legend, the reader is referred to the web version of this article.)

transgressively in channels that persisted in the same location for a long period of time. We favour the latter suggestion for the longest eskers because they are associated with the sectors of the ice sheet whose geometry was most stable during deglaciation, and because it does not require an abrupt and large quantity of meltwater and sediment to enter the drainage system. However, the maximum length of the esker-forming R-channels at a given ice margin could not be identified, because definitive ice-marginal indicators that can be directly linked to the eskers (e.g. fans) were not mapped.

The longest and least fragmented eskers are located in the Keewatin sector of the LIS, which experienced stable, gradual retreat. Conversely, the eskers of the Labrador sector are typically shorter and more fragmented, which we suggest reflects the more dynamic deglaciation experienced by this sector of the LIS.

Eskers are much straighter than has previously been assumed, with mean esker sinuosity at 1.06. This is an important constraint

for numerical models of subglacial channels and for understanding the discharge and velocity of meltwater through channels. Our data suggest that models and dye tracing experiments could overestimate sinuosity values for channels at the ice sheet scale.

We suggest that observations of very long, straight eskers indicate that they formed in conduits that maintained a stable position, perpendicular to the retreating ice margin. These eskers likely formed in conduits located in areas where the ice sheet geometry changed little during deglaciation and also where the hydraulic gradient was such that meltwater was drawn preferentially to those locations. These conduits existed at lower pressure than the surrounding system and so were able to capture drainage. This observation demonstrates that antecedent drainage conditions are an important factor in determining where water will drain in a retreating ice sheet.

Esker spacing is regular on the crystalline bedrock of the Canadian Shield. The spacing between esker-forming channels in three large study areas gives a mean value of 12.3 km (standard deviation 6.6 km) and this value is in agreement with numerical modelling (Boulton et al., 2007b, 2009; Hewitt, 2011). These models suggest that spacing should decrease when the supply of meltwater increases, which implies that as the LIS deglaciated, more meltwater was drained in channels which then filled with sediment to form eskers.

As the LIS deglaciated, eskers in the Keewatin and Labrador sectors became more densely spaced (between 12 and 9 ka BP in Keewatin and between 13 and 7.6 ka BP in Labrador). At the same time, the number of tributary eskers decreased. These observations suggest that the subglacial meltwater drainage systems around the ice divides evolved to become increasingly channelised as more meltwater became available.

An analysis of 11,562 eskers within the larger database reveals that they do not have a preferred up- or down-slope trend, indicating that conduits were close to ice overburden pressure. However, eskers trending uphill support the assertion that ice surface is an important control on esker and R-channel location.

Acknowledgements

References

Aylsworth, J.M., Shilts, W.W., 1989a. Bedforms of the Keewatin Ice-Sheet, Canada. Sediment. Geol. 62, 407—428.

Aylsworth, J.M., Shilts, W.W., 1989b. Glacial Features Around the Keewatin Ice Divide: Districts of Mackenzie and Keewatin. Geological Survey of Canada, Map 24-1987. 1:1,000,000.

Aylsworth, J.M., Shilts, W.W., Russell, H.A.J., Pyne, D.M., 2012. Eskers Around the Keewatin Ice Divide: Northwest Territories and Nunavut. Geological Survey of Canada, Open File, 7047.

Banerjee, I., McDonald, B.C., 1975. Nature of esker sedimentation. In: Jopling, A.V., McDonald, B.C. (Eds.), Glaciofluvial and Glacilacustrine Sedimentation. SEPM, Oklahoma, pp. 304—320.

Bartholomew, I., Nienow, P., Mair, D., Hubbard, A., King, M.A., Sole, A., 2010. Seasonal evolution of subglacial drainage and acceleration in a Greenland outlet glacier. Nat. Geosci. 3, 408—411.

Bolduc, A.M., 1992. The Formation of Eskers Based on Their Morphology, Stratigraphy and Lithologic Composition, Labrador, Canada (Unpublished Ph.D. thesis). Lehigh University.

Boulton, G.S., Clark, C.D., 1990. A highly mobile Laurentide ice sheet revealed by satellite images of glacial lineations. Nature 346, 813—817.

Boulton, G.S., Dobbie, K.E., Zatsepin, S., 2001. Sediment deformation beneath glaciers and its coupling to the subglacial hydraulic system. Quat. Int. 86, 3—28.

Boulton, G.S., Hagdorn, M., Maillot, P.B., Zatsepin, S., 2009. Drainage beneath ice sheets: groundwater-channel coupling, and the origin of esker systems from former ice sheets. Quat. Sci. Rev. 28, 621—638.

Boulton, G.S., Lunn, R., Vidstrand, P., Zatsepin, S., 2007a. Subglacial drainage by groundwater-channel coupling, and the origin of esker systems: part I-glaciological observations. Quat. Sci. Rev. 26, 1067—1090.

Boulton, G.S., Lunn, R., Vidstrand, P., Zatsepin, S., 2007b. Subglacial drainage by groundwater-channel coupling, and the origin of esker systems: part II-theory and simulation of a modern system. Quat. Sci. Rev. 26, 1091—1105.

Brennand, T.A., 1994. Macroforms, large bedforms and rhythmic sedimentary sequences in subglacial eskers, south-central Ontario - implications for esker genesis and meltwater regime. Sediment. Geol. 91, 9—55.

Brennand, T.A., 2000. Deglacial meltwater drainage and glaciodynamics: inferences from Laurentide eskers, Canada. Geomorphology 32, 263—293.

Brennand, T.A., Shaw, J., 1994. Tunnel channels and associated landforms, south-central Ontario: their implications for ice-sheet hydrology. Can. J. Earth Sci. 31, 505—522.

Brennand, T.A., Shaw, J., 1996. The Harricana glaciofluvial complex, Abitibi region, Quebec: its genesis and implications for meltwater regime and ice-sheet dynamics. Sediment. Geol. 102, 221—262.

Brown, V.H., Stokes, C.R., O'Cofaigh, C., 2011. The glacial geomorphology of the north-west sector of the Laurentide Ice Sheet. J. Maps 7, 409—428.

Burke, M.J., Brennand, T.A., Perkins, A.J., 2012. Transient subglacial hydrology of a thin ice sheet: insights from the Chasm esker, British Columbia, Canada. Quat. Sci. Rev. 58, 30—55.

Burke, M.J., Woodward, J., Russell, A.J., Fleisher, P.J., 2009. Structural controls on englacial esker sedimentation: Skeiðarárjökull, Iceland. Ann. Glaciol. 50, 85—92.

Burke, M.J., Woodward, J., Russell, A.J., Fleisher, P.J., Bailey, P.K., 2008. Controls on the sedimentary architecture of a single event englacial esker: Skeiðarárjökull, Iceland. Quat. Sci. Rev. 27, 1829—1847.

Burke, M.J., Woodward, J., Russell, A.J., Fleisher, P.J., Bailey, P.K., 2010. The sedimentary architecture of outburst flood eskers: a comparison of ground-penetrating radar data from Bering Glacier, Alaska and Skeiðarárjökull, Iceland. Bull. Geol. Soc. Am. 122, 1637—1645.

Carlson, A.E., Anslow, F.S., Obbink, E.A., LeGrande, A.N., Ullman, D.J., Licciardi, J.M., 2009. Surface-melt driven Laurentide Ice Sheet retreat during the early Holocene. Geophys. Res. Lett. L24502.

Carlson, A.E., LeGrande, A.N., Oppo, D.W., Came, R.E., Schmidt, G.A., Anslow, F.S., Licciardi, J.M., Obbink, E.A., 2008. Rapid early Holocene deglaciation of the Laurentide ice sheet. Nat. Geosci. 1, 620—624.

Carter, S.P., Blankenship, D.D., Young, D.A., Holt, J.W., 2009. Using radar-sounding data to identify the distribution and sources of subglacial water: application to Dome C, East Antarctica. J. Glaciol. 55, 1025—1040.

Clark, C.D., Evans, D.J.A., Khatwa, A., Bradwell, T., Jordan, C., Marsh, S., Mitchell, W., Bateman, M., 2004. Map and GIS database of glacial landforms and features related to the last British Ice Sheet. Boreas 33, 359—375.

Clark, C.D., Hughes, A.L.C., Greenwood, S.L., Jordan, C., Sejrup, H.P., 2012. Pattern and timing of retreat of the last British-Irish Ice Sheet. Quat. Sci. Rev. 44, 112—146.

Clark, C.D., Hughes, A.L.C., Greenwood, S.L., Spagnolo, M., Ng, F.S.L., 2009. Size and shape characteristics of drumlins, derived from a large sample, and associated scaling laws. Quat. Sci. Rev. 28, 677—692.

Clark, C.D., Knight, J.K., Gray, J.T., 2000. Geomorphological reconstruction of the Labrador sector of the Laurentide Ice Sheet. Quat. Sci. Rev. 19, 1343—1366.

Clark, P.U., Walder, J.S., 1994. Subglacial drainage, eskers, and deforming beds beneath the Laurentide and Eurasian ice sheets. Bull. Geol. Soc. Am. 106, 304—314.

Cuffey, K.M., Paterson, W.S.B., 2010. The Physics of Glaciers. Butterworth-Heinemann, Amsterdam; London.

Dunlop, P., Clark, C.D., 2006. The morphological characteristics of ribbed moraine. Quat. Sci. Rev. 25, 1668—1691.

Dyke, A.S., Dredge, L.A., Hodgson, D.A., 2005. North American deglacial marine- and lake-limit surfaces. Géogr. Phys. Quat. 59, 155—185.

Dyke, A.S., Moore, A., Robertson, L., 2003. Deglaciation of North America. Geological Survey of Canada, Open File, 1574.

Dyke, A.S., Prest, V.K., 1987. Late Wisconsinan and Holocene history of the Laurentide ice sheet. Géogr. Phys. Quat. 41, 237—263.

Flint, R.F., 1928. Eskers and crevasse fillings. Am. J. Sci. 15.

Flowers, G.E., Bjornsson, H., Palsson, F., 2003. New insights into the subglacial and periglacial hydrology of Vatnajokull, Iceland, from a distributed physical model. J. Glaciol. 49, 257—270.

Fricker, H.A., Scambos, T., Bindschadler, R., Padman, L., 2007. An active subglacial water system in West Antarctica mapped from space. Science 315, 1544—1548.

Fricker, H.A., Scambos, T., Carter, S., Davis, C., Haran, T., Joughin, I., 2010. Synthesizing multiple remote-sensing techniques for subglacial hydrologic mapping: application to a lake system beneath MacAyeal Ice Stream, West Antarctica. J. Glaciol. 56, 187—199.

Gleeson, T., Smith, L., Moosdorf, N., Hartmann, J., Dürr, H.H., Manning, A., van Beek, Ludovicus P.H., Jellinek, A.M., 2011. Mapping permeability over the surface of the Earth. Geophys. Res. Lett. 38, L02401.

Gorrell, G., Shaw, J., 1991. Deposition in an esker, bead and fan complex, Lanark, Ontario, Canada. Sediment. Geol. 72, 285—314.

Grasby, S.E., Chen, Z., 2005. Subglacial recharge into the Western Canadian Sedimentary Basin — impact of Pleistocene glaciation on basin hydrodynamics. Geol. Surv. Am. Bull. 117, 500—514.

Gulley, J.D., 2009. Structural control of englacial conduits in the temperate Matanuska Glacier, Alaska, USA. J. Glaciol. 55, 681—690.

Gulley, J.D., Benn, D.I., 2007. Structural control of englacial drainage systems in Himalayan debris-covered glaciers. J. Glaciol. 53, 399—412.

Gulley, J.D., Benn, D.I., Müller, D., Luckman, A., 2009a. A cut-and-closure origin for englacial conduits in uncrevassed regions of polythermal glaciers. J. Glaciol. 55, 66—80.

Gulley, J.D., Benn, D.I., Screaton, E., Martin, J., 2009b. Mechanisms of englacial conduit formation and their implications for subglacial recharge. Quat. Sci. Rev. 28, 1984—1999.

Gustavson, T.C., Boothroyd, J.C., 1987. A depositional model for outwash, sediment sources, and hydrologic characteristics, Malaspina Glacier, Alaska: a modern analog of the southeastern margin of the Laurentide Ice Sheet. Bull. Geol. Soc. Am. 99, 187.

Hättestrand, C., Clark, C.D., 2006. The glacial geomorphology of Kola Peninsula and adjacent areas in the Murmansk Region, Russia. J. Maps 30, 30—42.

Hewitt, I.J., 2011. Modelling distributed and channelized subglacial drainage: the spacing of channels. J. Glaciol. 57, 302—314.

Hewitt, I.J., 2013. Seasonal changes in ice sheet motion due to melt water lubrication. Earth Planet. Sci. Lett. 371—372, 16—25.

Hillaire-Marcel, C., Occhietti, S., 1980. Chronology, paleogeography, and paleoclimatic significance of the late and postglacial events in eastern Canada. Z. Geomorphol. 24, 373—392.

Hillier, J.K., Smith, M.J., Clark, C.D., Stokes, C.R., Spagnolo, M., 2013. Subglacial bedforms reveal an exponential size-frequence distribution. Geomorphology 190, 82—91.

Jones, B.M., Grosse, G., Arp, C.D., Jones, M.C., Walter Anthony, K.M., Romanovsky, V.E., 2011. Modern thermokarst lake dynamics in the continuous permafrost zone, northern Seward Peninsula, Alaska. J. Geophys. Res. Biogeosci. 116.

Joughin, I., Das, S.B., King, M.A., Smith, B.E., Howat, I.M., Moon, T., 2008. Seasonal speedup along the western flank of the Greenland Ice Sheet. Science 320, 781—783.

Kleman, J., 1994. Preservation of landforms under ice sheets and ice caps. Geomorphology 9, 19—32.

Kleman, J., Glasser, N.F., 2007. The subglacial thermal organisation (STO) of ice sheets. Quat. Sci. Rev. 26, 585—597.

Kleman, J., Hättestrand, C., 1999. Frozen-bed Fennoscandian and Laurentide ice sheets during the Last Glacial Maximum. Nature 402, 63—66.

Lagerbäck, R., Robertsson, A.-M., 1988. Kettle holes - stratigraphical archives for Weichselian geology and palaeoenvironment in northernmost Sweden. Boreas 17, 439—468.

Lewis, S.M., Smith, L., 2009. Hydrologic drainage of the Greenland Ice Sheet. Hydrol. Process. 23, 2004—2011.

Livingstone, S.J., Clark, C.D., Tarasov, L., 2013. Modelling North American palaeo-subglacial lakes and their meltwater drainage pathways. Earth Planet. Sci. Lett. 375, 13—33.

Lliboutry, L.A., 1969. Contribution à la théorie des ondes glaciaires. Can. J. Earth Sci. 6, 943—956.

Lundqvist, J.A.N., 1997. Structure and rhythmic pattern of glaciofluvial deposits north of Lake Vänern, south-central Sweden. Boreas 26, 127—140.

Makaske, B., 2001. Anastomosing rivers: a review of their classification, origin and sedimentary products. Earth Sci. Rev. 53, 149—196.

Margold, M., Jansson, K., Kleman, J., Stroeven, A., 2011. Glacial meltwater landforms of central British Columbia. J. Maps 2011, 486—506.

Margold, M., Jansson, K.N., Kleman, J., Stroeven, A.P., Clague, J.J., 2013. Retreat pattern of the Cordilleran Ice Sheet in central British Columbia at the end of the last glaciation reconstructed from glacial meltwater landforms. Boreas 42, 830—847.

Marshall, S.J., Clark, P.U., 2002. Basal temperature evolution of North American ice sheets and implications for the 100-kyr cycle. Geophys. Res. Lett. 29, 2214.

Mooers, H.D., 1989. On the formation of the tunnel valleys of the Superior Lobe, central Minnesota. Quat. Res. 32, 24—35.

Nienow, P., Sharp, M., Willis, I., 1998. Seasonal changes in the morphology of the subglacial drainage system, Haut Glacier d'Arolla, Switzerland. Earth Surf. Process. Landf. 23, 825—843.

Nienow, P.W., Sharp, M., Willis, I.C., 1996. Velocity-discharge relationships derived from dye tracer experiments in glacial meltwaters: implications for subglacial flow conditions. Hydrol. Process. 10, 1411—1426.

Peltier, W.R., 2004. Global glacial isostacy and the surface of the ice-age Earth: the ICE-5G (VM2) model and GRACE. Annu. Rev. Earth Planet. Sci. 32, 111—149.

Prest, V.K., Grant, D.R., Rampton, V.N., 1968. Glacial Map of Canada. Geological Survey of Canada, Map 1253A. 1:5,000,000.

Price, R.J., 1966. Eskers near the Casement glacier, Alaska. Geogr. Ann. Ser. A Phys. Geogr. 48, 111—125.

Price, R.J., 1969. Moraines, sandar, kames and eskers near Breiðamerkurjökull, Iceland. Trans. Inst. Br. Geogr. 46, 17—43.

Richards, K., Sharp, M., Arnold, N., Gurnell, A., Clark, M., Tranter, M., Nienow, P., Brown, G., Willis, I., Lawson, W., 1996. An integrated approach to modelling hydrology and water quality in glacierized catchments. Hydrol. Process. 10, 479—508.

Röthlisberger, H., 1972. Water pressure in intra-and subglacial channels. J. Glaciol. 11, 177—203.

Schoof, C., 2010. Ice-sheet acceleration driven by melt supply variability. Nature 468, 803—806.

Schuler, T.V., Fischer, U.H., 2009. Modeling the diurnal variation of tracer transit velocity through a subglacial channel. J. Geophys. Res. 114, F04017.

Schumm, S., 1963. Sinuosity of alluvial rivers on the Great Plains. Geol. Soc. Am. Bull. 74, 1089—1100.

Shakun, J.D., Clark, P.U., He, F., Marcott, S.A., Mix, A.C., Liu, Z., Otto-Bliesner, B., Schmittner, A., Bard, E., 2012. Global warming preceded by increasing carbon dioxide concentrations during the last deglaciation. Nature 484, 49—54.

Shilts, W.W., Aylsworth, J.M., Kaszycki, C.A., Klassen, R.A., 1987. Canadian shield. In: Graf, W.L. (Ed.), Geomorphic Systems of North America. Geological Society of America, Boulder, Colorado, pp. 119—161. Centennial Special Volume. 2.

Shoemaker, E.M., 1986. Subglacial hydrology for an ice sheet resting on a deformable aquifer. J. Glaciol. 32, 20—30.

Shreve, R.L., 1972. Movement of water in glaciers. J. Glaciol. 11, 205—214.

Shreve, R.L., 1985a. Esker characteristics in terms of glacier physics, Katahdin esker system, Maine. Bull. Geol. Soc. Am. 96, 639—646.

Shreve, R.L., 1985b. Late Wisconsin ice-surface profile calculated from esker paths and types, Katahdin esker system, Maine. Quat. Res. 23, 27—37.

Sissons, J.B., 1958. Sub-glacial stream erosion in Southern Northumberland. Scott. Geogr. Mag. 74, 163—174.

Smith, L.C., Sheng, Y., MacDonald, G.M., 2007. A first pan-Arctic assessment of the influence of glaciation, permafrost, topography and peatlands on northern hemisphere lake distribution. Permafr. Periglac. Process. 18, 201—208.

Smith, L.C., Sheng, Y., MacDonald, G.M., Hinzman, L.D., 2005. Disappearing Arctic Lakes. Science 308, 1429.

Spagnolo, M., Clark, C.D., Hughes, A.L.C., 2012. Drumlin relief. Geomorphology 153, 179—191.

Spagnolo, M., Clark, C.D., Ely, J.C., Stokes, C.R., Anderson, J.B., Andreassen, K., Graham, A.G.C., King, E.C., 2014. Size, shape and spatial arrangement of mega-scale glacial lineations from a large and diverse dataset. Earth Surf. Process. Landf. 39, 1432—1448.

St-Onge, D.A., 1984. Surficial deposits of the Redrock Lake area, District of Mackenzie. Current Research: Part A. Geological Survey of Canada Paper, 84—01A, 271-278.

Stokes, C.R., Clark, C.D., 2003a. The Dubawnt Lake palaeo ice stream: evidence for dynamic ice sheet behaviour on the Canadian Shield and insights regarding the controls on ice stream location and vigour. Boreas 32, 263—279.

Stokes, C.R., Clark, C.D., 2003b. Laurentide ice streaming on the Canadian Shield: a conflict with the soft-bedded ice stream paradigm? Geology 31, 347—350.

Stokes, C.R., Clark, C.D., Storrar, R.D., 2009. Major changes in ice stream dynamics during deglaciation of the north-western margin of the Laurentide Ice Sheet. Quat. Sci. Rev. 28, 721—738.

Stokes, C.R., Spagnolo, M., Clark, C.D., O'Cofaigh, C., Lian, O.B., Dunstone, R.B., 2013. Formation of mega-scale glacial lineations on the Dubawnt Lake Ice Stream bed: 1. size, shape and spacing from a large remote sensing dataset. Quat. Sci. Rev. 77, 190—209.

Storrar, R.D., Stokes, C.R., Evans, D.J.A., 2013. A map of Canadian eskers from Landsat satellite imagery. J. Maps 9, 456—473.

Storrar, R.D., Stokes, C.R., Evans, D.J.A., 2014. Increased channelization of subglacial drainage during deglaciation of the Laurentide Ice Sheet. Geology 42, 239—242.

Sundal, A.V., Shepherd, A., Nienow, P., Hanna, E., Palmer, S., Huybrechts, P., 2011. Melt-induced speed-up of Greenland ice sheet offset by efficient subglacial drainage. Nature 469, 521—524.

Syverson, K.M., Gaffield, S.J., Mickelson, D.M., 1994. Comparison of esker morphology and sedimentology with former ice-surface topography, Burroughs Glacier, Alaska. Geol. Soc. Am. Bull. 106, 1130—1142.

Tulaczyk, S.M., Kamb, B., Engelhardt, H.F., 2000. Basal mechanics of Ice Stream B. II. Plastic-undrained bed model. J. Geophys. Res. 105, 483—494.

Walder, J.S., Fowler, A., 1994. Channelized subglacial drainage over a deformable bed. J. Glaciol. 40, 3—15.

Warren, W.P., Ashley, G.M., 1994. Origins of the ice-contact stratified ridges (eskers) of Ireland. J. Sediment. Res. 64, 433—499.

Weertman, J., 1972. General theory of water flow at the base of a glacier or ice sheet. Rev. Geophys. 10, 287—333.

Werder, M.A., Hewitt, I.J., Schoof, C.G., Flowers, G.E., 2013. Modeling channelized and distributed subglacial drainage in two dimensions. J. Geophys. Res. Earth Surf. 118, 2140—2158.

Wheeler, J.O., Hoffman, P.F., Card, K.D., Davidson, A., Sanford, B.V., Okulitch, A.V., Roest, W.R., 1996. Geological Map of Canada. Geological Survey of Canada, map 1860A.

Wingham, D.J., Siegert, M.J., Shepherd, A., Muir, A.S., 2006. Rapid discharge connects Antarctic subglacial lakes. Nature 440, 1033—1036.

Wright, H.E., 1973. Tunnel valleys, glacial surges, and subglacial hydrology of the Superior Lobe, Minnesota. Geol. Soc. Am. Mem. 136, 251—276.

Zwally, H.J., Abdalati, W., Herring, T., Larson, K., Saba, J., Steffen, K., 2002. Surface melt-induced acceleration of Greenland ice-sheet flow. Science 297, 218—222.